Eidgenössische Technische Hochschule Zürich

Ecole polytechnique fédérale de Zurich
Politecnico federale di Zurigo
Swiss Federal Institute of Technology Zurich

The *hp*-Version of the Streamline Diffusion Finite Element Method in Two Space Dimensions

K. Gerdes*, J.M. Melenk, D. Schötzau and C. Schwab

Research Report No. 99-17
September 1999

Seminar für Angewandte Mathematik
Eidgenössische Technische Hochschule
CH-8092 Zürich
Switzerland

*Department of Mathematics, Chalmers University, SE-412 96 Göteborg, Sweden

The *hp*-Version of the Streamline Diffusion Finite Element Method in Two Space Dimensions

K. Gerdes*, J.M. Melenk, D. Schötzau and C. Schwab

Seminar für Angewandte Mathematik
Eidgenössische Technische Hochschule
CH-8092 Zürich
Switzerland

Research Report No. 99-17 September 1999

Abstract

The Streamline Diffusion Finite Element Method (SDFEM) for a two dimensional convection-diffusion problem is analyzed in the context of the *hp*-version of the Finite Element Method (FEM). It is proved that the appropriate choice of the SDFEM parameters leads to stable methods on the class of "boundary layer meshes" which may contain anisotropic needle elements of arbitrarily high aspect ratio. Consistency results show that the use of such meshes can resolve layer components present in the solutions at robust exponential rates of convergence. We confirm these theoretical results in a series of numerical examples.

Keywords: Streamline Diffusion Methods, *hp* Finite Element Methods

Subject Classification (1991): 65N30

*Department of Mathematics, Chalmers University, SE-412 96 Göteborg, Sweden

1. Introduction

Standard Galerkin Finite Element Methods (FEM) for convection-dominated convection-diffusion problems are known to produce often wildely oscillatory solutions due to intrinsic stability problems in the schemes. To circumvent these stability problems the Streamline Diffusion Finite Element Method (SDFEM) was introduced by T. Hughes, C. Johnson and their coworkers. We mention here only the pioneering work [4, 6, 7, 11, 12, 13] and the references there. In the meantime, numerous papers have appeared where the SDFEM and related Streamline Upwind Petrov Galerkin (SUPG) techniques have been applied successfully to incompressible fluid flow problems and to solid mechanics problems with analogous mathematical structure (see, e.g., [8, 29, 30] and the references there).
However, all these approaches were mainly concerned with the h-version FEM where convergence is achieved by refining the mesh $\mathcal{T}$ at fixed, low polynomial degree p. The convergence rates were consequently at best *algebraic*. In the 1980ies, the p- and hp-FEM were introduced by I. Babuška, B.A. Szabó and their coworkers, and it was shown that the hp-FEM achieves *exponential convergence* for elliptic problems with *piecewise analytic* solutions (cf. the survey paper [1] and the references therein).
The hp-version of the SDFEM for convection-dominated problems in one space dimension was analyzed in [17]. There, *robust exponential convergence* of the hp-SDFEM (and of the hp-Galerkin FEM) is proved in global norms (mainly the L^2 norm and the "energy norm", cf. (2.14)) provided that boundary layers and fronts in the solution are resolved. Whereas in the h-version FEM this requirement of scale resolution amounts to the use of anisotropic, so-called Shishkin meshes (cf. [20, 22]), in the hp-version context this can be achieved very efficiently by inserting anisotropic needle elements of the proper width into the layer (see, e.g., [15, 16, 17, 18, 24, 27]). Furthermore, the behavior of the hp-SDFEM was investigated under the assumption that layers are not resolved which may happen, for example, when the precise location of the layer is unknown. In this case, the hp-SDFEM can lead to robust exponential convergence on compact subsets upstream of the layer/shock while the performance of the hp-Galerkin FEM is poor throughout the domain. This is important in adaptive schemes that try to locate and resolve the layers. In the one dimensional case, a complete convergence analysis of the hp-SDFEM was possible in [17] because precise regularity results for the exact solution were available.
In two space dimensions, however, the regularity theory is much more complex and analytic regularity to prove robust exponential convergence does not seem to be available at present. Usually, the regularity of the exact solution is described by means of asymptotic expansions. There, the solution is decomposed into a smooth (piecewise analytic) part, a layer part, and a (small) remainder. While the regularity of the smooth and layer parts are well understood, it is the analytic regularity of the remainder, containing, for example, corner layers, that is not very well understood. Nevertheless, mesh design principles for the robust exponential approximation of the dominant solution components, the smooth part and the layer part, are available [18].
In the present work we extend the hp-SDFEM to convection-diffusion problems in two space dimensions and show that:

1. The appropriate choice of the SDFEM parameters leads to stable methods on boundary layer meshes which may contain anisotropic needle elements of arbitrarily high aspect ratio.

2. Boundary layer meshes can resolve the layer components present in the exact solution; the SDFEM based on such boundary layer meshes can lead to exponential rates of convergence where the constants depend only very weakly on the perturbation parameter.

3. The SDFEM on shape regular meshes yields optimal *hp*-convergence rates for smooth solutions.

The performance of the *hp*-SDFEM is studied in a series of numerical examples. We illustrate that the *hp*-version mesh design principles indeed permit the resolution of localized small scale features such as boundary layers and lead to robust exponential convergence in the global energy norm. Under the assumption that the layers are not resolved, we can still observe exponential rates of convergence upstream of the layer, in agreement with the corresponding results in one dimension [17]. We point out, however, that this convergence behavior upstream is fairly sensitive to the choice of the SDFEM parameters.
The outline of the paper is as follows: In Section 2 we present our model convection-diffusion problem and review the SDFEM formulation in the *hp*-context. In Section 3 we introduce the class of "boundary layer meshes" and discuss the *hp*-approximation of layer components on such meshes. Section 4 is devoted to the stability analysis of the SDFEM on boundary layer meshes. In Section 5 we prove consistency results for the *hp*-SDFEM and show that smooth and layer components can be resolved at robust exponential rates of convergence. On shape regular meshes optimal *hp* error bounds are derived for smooth solutions. We conclude our presentation with numerical results in Section 6.
Standard notations and conventions are followed in this paper. For a domain D the Lebesgue space of square integrable functions is denoted $L^2(D)$. We write $(\cdot,\cdot)_D$ for the $L^2(D)$ inner product where the index D is omitted if clear from the context. The corresponding norm is $\|\cdot\|_{L^2(D)}$. $L^\infty(D)$ is the space of all bounded functions equipped with the supremum norm $\|\cdot\|_\infty$. The Sobolev spaces of order $k \geq 0$ are denoted by $H^k(D)$. We write $\|\cdot\|_{H^k(D)}$ and $|\cdot|_{H^k(D)}$ for the corresponding norms and semi-norms. $H_0^1(D)$ is the space of $H^1(D)$-functions with vanishing trace on the boundary ∂D of D. The Sobolev spaces of L^∞-functions are denoted by $W^{k,\infty}(\Omega)$. We use the notation $\mathcal{Q}^p(D)$ for the set of all polynomials of degree $\leq p$ in each variable and $\mathcal{P}^p(D)$ for the set of all polynomials of total degree $\leq p$. In the following we denote by $c, C, C_1, C_2, \ldots$ generic constants not necessarily identical at different places but always independent of the meshwidths, the polynomial degrees, and the singular perturbation parameter ε. Similarly, the constant σ arising in expressions of the type $e^{-\sigma p}$ is independent of the polynomial degree p and the perturbation parameter ε but not necessarily the same in different instances.

2. The Streamline Diffusion Finite Element Method (SDFEM)

In this section we introduce the SDFEM discretization of convection-diffusion problems based on *hp* Finite Element spaces.

2.1. The Convection-Diffusion Problem

In a curvilinear Lipschitzian polygon $\Omega \subset \mathbb{R}^2$ we consider the convection-diffusion problem

$$-\varepsilon \Delta u(x) + \vec{a}(x) \cdot \nabla u(x) + b(x)u(x) = f(x) \qquad \text{in } \Omega, \tag{2.1}$$

$$u = 0 \qquad \text{on } \partial\Omega. \tag{2.2}$$

Here, the parameter $\varepsilon \in (0, 1]$ may approach zero, the right-hand side f is in $L^2(\Omega)$, and the coefficients $\vec{a} = (a_1, a_2)$ and b are assumed to be bounded, differentiable and to satisfy

$$b(x) - \frac{1}{2}\nabla \cdot \vec{a}(x) \geq \mu > 0, \qquad x \in \Omega. \tag{2.3}$$

Condition (2.3) guarantees the stability and the unique solvability of (2.1), (2.2) for all $\varepsilon \in (0, 1]$. The standard weak formulation of (2.1), (2.2) is:
Find $u \in H_0^1(\Omega)$ such that

$$\varepsilon \int_\Omega \nabla u \cdot \nabla v dx + \int_\Omega (\vec{a} \cdot \nabla u + bu)v dx = \int_\Omega f v dx \qquad \forall v \in H_0^1(\Omega). \tag{2.4}$$

2.2. Finite Element Spaces

In order to solve (2.1), (2.2) numerically by a Finite Element Method the infinite dimensional space $H_0^1(\Omega)$ in (2.4) is replaced by a finite dimensional FE-space of functions which are piecewise mapped polynomials on a mesh $\mathcal{T}$:
A mesh $\mathcal{T}$ on $\Omega \subset \mathbb{R}^2$ consists of curvilinear quadrilateral and/or triangular elements $\{K\}$ satisfying the following standard assumptions:

(i) The elements $\{K\}$ partition the domain, i.e., they are open, pairwise disjoint and there holds $\overline{\Omega} = \cup_{K \in \mathcal{T}} \overline{K}$.

(ii) Each element K is the image of the generic reference element $\hat{K}$ which is either the reference triangle $\hat{T} = \{(x, y) : 0 < x < 1,\ 0 < y < x\}$ or the reference square $\hat{Q} = (0, 1)^2$, i.e., with $K \in \mathcal{T}$ there is associated an element mapping $F_K : \hat{K} \to K$. F_K is an analytic diffeomorphism in a neighborhood of $\overline{\hat{K}}$ with $\det DF_K > 0$ on $\overline{\hat{K}}$.

(iii) The intersection $\overline{K} \cap \overline{K'}$ of two elements K and K' is either empty, one common vertex or one entire side. (Vertices and sides are the images of the vertices and sides of the reference element $\hat{K}$ under F_K.)

(iv) The parametrization is the same "from both sides": Let $\gamma = \overline{K} \cap \overline{K'}$ be the common side of K and K' with endpoints P_1 and P_2. Then for any point P on γ we have $\mathrm{dist}(F_K^{-1}(P), F_K^{-1}(P_i))/l_K = \mathrm{dist}(F_{K'}^{-1}(P), F_{K'}^{-1}(P_i))/l_{K'}$ for $i = 1, 2$ where l_K and $l_{K'}$ denote the lengths of the corresponding edges of the reference elements of K and K', respectively.

We denote by $h_{K,max}$ and $h_{K,min}$ the maximal and minimal lengths of the sides of $K \in \mathcal{T}$. The mesh $\mathcal{T}$ is called *shape regular* if

(i) There is a constant $\kappa > 0$ independent of the elements and the partition such that $h_{K,max} \leq \kappa h_{K,min}$.

(ii) On $\overline{\hat{K}}$ we have $\|D^\beta F_K\|_\infty \leq C h_{K,max}$ for multi-indices β with $1 \leq |\beta| \leq 2$ and $C_1 h_{K,min}^2 \leq \det DF_K \leq C_2 h_{K,max}^2$ with constants C, C_1 and C_2 independent of the elements.

$\mathcal{T}$ is called *affine* if the element mappings F_K are affine transformations.
Let now $\underline{p} = \{p_K : K \in \mathcal{T}\}$ be a degree vector on $\mathcal{T}$ which associates with each element $K \in \mathcal{T}$ a polynomial degree p_K. The space $S^{\underline{p}}(\mathcal{T})$ of piecewise mapped polynomials is then defined as follows:

$$S^{\underline{p}}(\mathcal{T}) := \{u \in H^1(\Omega) : u|_K \circ F_K \in \mathcal{S}^{p_K}(\hat{K}),\ \forall K \in \mathcal{T}\}. \tag{2.5}$$

Here, the generic polynomial space $\mathcal{S}^p(\hat{K})$ is to be understood as $\mathcal{Q}^p(\hat{Q})$ if $\hat{K} = \hat{Q}$ and as $\mathcal{P}^p(\hat{T})$ if $\hat{K} = \hat{T}$. Further, we define $S_0^{\underline{p}}(\mathcal{T}) := S^{\underline{p}}(\mathcal{T}) \cap H_0^1(\Omega)$. If $p_K = p$ for all $K \in \mathcal{T}$, we simply write $S^p(\mathcal{T})$ and $S_0^p(\mathcal{T})$, respectively.

2.3. SDFEM Discretization

The standard Galerkin Finite Element Method for (2.1), (2.2) is:
Find $U \in S_0^{\underline{p}}(\mathcal{T})$ such that

$$B(U,V) := \varepsilon \int_\Omega \nabla U \cdot \nabla V dx + \int_\Omega (\vec{a} \cdot \nabla U + bU) V dx = F(V) := \int_\Omega f V dx \tag{2.6}$$

for all $V \in S_0^{\underline{p}}(\mathcal{T})$.
To improve the stability of the scheme (2.6), the test function V is replaced by a test function "upwinded" in stream direction $\vec{a}$ given on each element K by $V|_K + \delta_K \rho_K (\vec{a} \cdot \nabla V)|_K$ where $\rho_K \geq 0$ is a mesh-dependent parameter (depending on $h_{K,max}$, $h_{K,min}$ and p_K) and $\delta_K \geq 0$ is a user-specified parameter to be selected later on. This yields the SDFEM formulation:

$$\text{Find } U \in S_0^{\underline{p}}(\mathcal{T}) \text{ such that } B_{SD}(U,V) = F_{SD}(V) \text{ for all } V \in S_0^{\underline{p}}(\mathcal{T}) \tag{2.7}$$

where

$$B_{SD}(U,V) := B(U,V) + \sum_{K \in \mathcal{T}} \delta_K \rho_K \int_K (-\varepsilon \Delta U + \vec{a} \cdot \nabla U + bU)(\vec{a} \cdot \nabla V) dx, \tag{2.8}$$

$$F_{SD}(U,V) := F(V) + \sum_{K \in \mathcal{T}} \delta_K \rho_K \int_K f(\vec{a} \cdot \nabla V) dx. \tag{2.9}$$

If $f \in L^2(\Omega)$, the exact solution u of (2.1), (2.2) satisfies $B_{SD}(u,V) = F_{SD}(V)$ for all $V \in S_0^{\underline{p}}(\mathcal{T})$ and hence there holds the orthogonality property

$$B_{SD}(U-u,V) = 0 \qquad \forall V \in S_0^{\underline{p}}(\mathcal{T}). \tag{2.10}$$

We assume the SDFEM parameters $\{\delta_K\}$ and $\{\rho_K\}$ to be given by

$$0 \leq \delta_K \leq \delta_0, \qquad \rho_K^2 = \frac{1}{p_K^{2\alpha}} \frac{h_{K,min}^2 h_{K,max}^2}{h_{K,max}^2 + h_{K,min}^2} \tag{2.11}$$

for some constants $\delta_0 > 0$ and $\alpha \geq 0$. We will make use of the following short-hand notation

$$h_K^2 := \frac{h_{K,min}^2 h_{K,max}^2}{h_{K,max}^2 + h_{K,min}^2}, \qquad K \in \mathcal{T}. \tag{2.12}$$

We will come back to the choice of the parameter α in our numerical experiments ahead. We note that the parameter $\delta_K = 0$ is not excluded in (2.11) and leads to the standard Galerkin FEM (2.6). In order to be able to analyze the "true" SDFEM, it will be convenient to assume occasionally the following non-degeneracy condition:

$$\exists \underline{\delta} > 0 \quad \text{such that } \delta_K \geq \underline{\delta} \qquad \forall K \in \mathcal{T}. \tag{2.13}$$

Our analysis will be performed in the framework of the "energy norm" $\|\cdot\|_E$ and mesh-dependent SDFEM norm $\|\cdot\|_{SD}$ given on $H_0^1(\Omega)$ as:

$$\|u\|_E^2 := \varepsilon \|\nabla u\|_{L^2(\Omega)}^2 + \mu \|u\|_{L^2(\Omega)}^2, \qquad \|u\|_{SD}^2 := \|u\|_E^2 + \sum_{K \in \mathcal{T}} \delta_K \rho_K \|\vec{a} \cdot \nabla u\|_{L^2(K)}^2. \tag{2.14}$$

Remark 2.1 In the subsequent analysis the parameters $\{\rho_K\}$ in (2.11) can equivalently be chosen as $\rho_K^2 = \frac{h_{K,min}^2}{p_K^{2\alpha}}$ because there holds $h_K \sim h_{K,min}$ by the standard two-sided bound $\frac{1}{2}\min\{a,b\} \leq \frac{ab}{a+b} \leq \min\{a,b\}$, valid for all a, $b > 0$.

3. Approximation on Boundary Layer Meshes

Due to the singular perturbation parameter ε solutions of (2.1), (2.2) exhibit boundary layer phenomena. The numerical approximation of these layers requires carefully designed meshes with anisotropic needle elements. In Section 3.2 the class of "boundary layer meshes" is introduced and in Section 3.3 it is shown that layers can be resolved on such meshes at exponential rates of convergence.

3.1. Properties of the Solutions

For the design of *hp* methods for (2.1), (2.2), it is important to have precise information about the solution behavior, that is, to have some regularity theory. The best tool available at present for describing the regularity are asymptotic expansions. There, the solution u is decomposed in a number of components, typically in the form

$$u = u_{smooth} + u_{layer} + u_{rem}. \tag{3.1}$$

Each solution component accounts for a different feature of the solution. In practice, the "smooth" part is piecewise analytic. The "layer" part consists of (possibly several) components which have a typical layer behavior: With respect to a special, fitted coordinate system (r, s) the layer component $u_{layer} = u_{layer}(r, s)$ behaves smoothly in the variable s but decays sharply in the other variable r. From an analysis of the simpler one dimensional case in [16, 17] and the related reaction-diffusion equation in two dimensions, [18], we can expect the layer parts to satisfy the following regularity properties:

Definition 3.1 *An analytic function $u = u(r, s)$ is said to be of* layer type *with length scale $l > 0$ if there are constants C, γ, $d > 0$ such that*

$$|\partial_r^m \partial_s^n u(r,s)| \leq C\gamma^{m+n} n! \max\{m, l^{-1}\}^m e^{-dr/l}, \qquad m, n \in \mathbb{N}_0, r > 0. \tag{3.2}$$

For the solutions of (2.1), (2.2) it is known that only two length scales l arise: $l = O(\varepsilon)$, giving so-called *exponential layers* and $l = O(\varepsilon^{1/2})$ for the so-called *parabolic layers*.
For such small length scales, we see that Definition 3.1 reflects the typical, anisotropic behavior of layers, namely, the rapid decay in one direction (here: for $r \to \infty$) and the fact that successive differentiation with respect to the variable r produces negative powers of the length scale on the one hand and a smooth (here: analytic) behavior in the other direction.
Layers appear as *boundary layers* near the outflow boundary $\Gamma_+ = \{x \in \partial\Omega \,|\, \vec{a}(x) \cdot \vec{n}(x) > 0\}$. There, the fitted coordinate system (r, s) is given by $r = \operatorname{dist}(x, \Gamma_+)$ and s is the arc-length parameter for Γ_+. The layers near Γ_+ are of exponential type. A similar situation holds for the characteristic part $\Gamma_0 = \{x \in \partial\Omega \,|\, \vec{a}(x) \cdot \vec{n}(x) = 0\}$, where parabolic layers are present. Another instance of parabolic layers is given by internal layers, caused by unsmoothness of the data near the inflow boundary $\Gamma_- = \{x \in \partial\Omega \,|\, \vec{a}(x) \cdot \vec{n}(x) < 0\}$. The remainder u_{rem} is defined such that (3.2) holds true once the smooth part u_{smooth} and the layer part u_{layer} are defined by means of asymptotic analysis. Little can be found in the literature about the regularity of u_{rem} (we hint at some of the difficulties by pointing out that in the case of a polygonal domain Ω, the solution has to exhibit corner singularities which can interact with boundary layers near some of the vertices). Fortunately, the remainder u_{rem} is in practice small and the components u_{smooth}, u_{layer} do indeed capture the dominant features of the solution u. In our analysis, we will therefore neglect the effects of the u_{rem}.

3.2. Boundary Layer Meshes

We introduce the class of "boundary layer meshes" that are designed to resolve layer components arising in solutions of (2.1), (2.2):

Definition 3.2 *A mesh $\mathcal{T}$ is called* boundary layer mesh *if for each element $K \in \mathcal{T}$ there exists a triangle $\hat{R}_K = \{(\xi, \eta) : 0 < \xi < h_x,\ 0 < \eta < \frac{h_y}{h_x}\xi\}$ or a rectangle $\hat{R}_K = (0, h_x) \times (0, h_y)$ such that the mapping $\tilde{F}_K(\xi, \eta) := F_K(\frac{\xi}{h_x}, \frac{\eta}{h_y})$, $(\xi, \eta) \in \overline{\hat{R}_K}$, satisfies on $\overline{\hat{R}_K}$*

$$C_1^{-1} \leq \det D\tilde{F}_K \leq C_1, \qquad \|D^\beta \tilde{F}_K\|_\infty \leq C_2 C_{\tilde{F}}^{|\beta|} |\beta|! \qquad \forall \text{ multi-indices } \beta \in \mathbb{N}_0^2 \tag{3.3}$$

with constants C_1, C_2 and $C_{\tilde{F}}$ independent of the elements.

Definition 3.2 formalizes the idea that for boundary layer meshes the element mappings F_K can be factorized into two transformations F_1 and $\tilde{F}_K$,

$$F_K(\hat{x}, \hat{y}) = \tilde{F}_K \circ F_1(\hat{x}, \hat{y}), \qquad F_1(\hat{x}, \hat{y}) = \begin{pmatrix} h_x & 0 \\ 0 & h_y \end{pmatrix} \begin{pmatrix} \hat{x} \\ \hat{y} \end{pmatrix}. \tag{3.4}$$

This is indicated in Figure 1. The scaling and anisotropy properties of the element K are coded into the map F_1, while $\tilde{F}_K$ is completely independent of these issues due to (3.3).

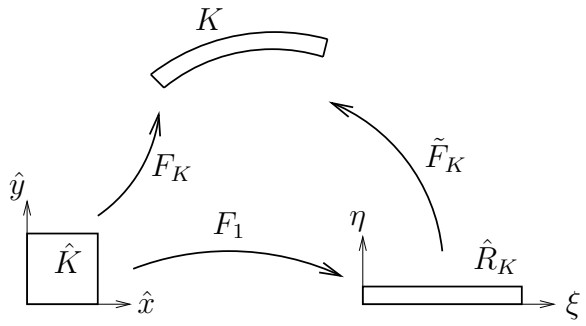

Figure 1: The factorization of the element mapping in boundary layer meshes.

The rather technical assumptions in (3.3) may be difficult to check in practice. A possibility to construct boundary layer meshes is the use of a macro-element technique. This approach is based on certain two-level families of meshes: We start with a macroscopic shape regular mesh $\mathcal{T}_m = \{M\}$. Some of these macro-element patches M are now further partitioned by mapping a corresponding refinement $\hat{\mathcal{T}}$ of the reference element into M with the element transformation F_M. We will be interested in the following reference patches $\hat{\mathcal{T}}$ which are defined in terms of additional parameters such as polynomial degrees p, length scales l, grading factors q and number of layers L (cf. Fig. 2):

(P1) The *trivial patch*: $\hat{\mathcal{T}} = \hat{K}$.

(P2) The *two-element patch*: $\hat{\mathcal{T}}_{\kappa pl} = \{(0, \kappa pl) \times (0,1), (\kappa pl, 1) \times (0,1)\}$.

(P3) The *geometric patch*: The reference element $\hat{K}$ is refined geometrically and anisotropically towards the line $x = 0$ with grading factor $q \in (0,1)$ and a number of layers $L \in \mathbb{N}_0$ such that $q^L \approx l$. That is, the mesh is given as $\hat{\mathcal{T}} = \{(x_{i+1}, x_i) \times (0,1) \,|\, i = 0, \ldots, L+1\}$ where $x_{L+1} = 0$ and $x_i = q^i$ for $i \in \{1, \ldots, L\}$.

(P4) The *tensor product patch*: For two length scales l_1, l_2 and grading factor $q \in (0,1)$ let L_1, $L_2 \in \mathbb{N}_0$ such that $q^{L_1} \approx l_1$, $q^{L_2} \approx l_2$. Then the reference element $\hat{K}$ is refined geometrically towards the lines $x = 0$ and $y = 0$ with L_1 layers in the x-direction and L_2 layers in the y-direction. That is, the mesh is given as $\hat{\mathcal{T}} = \{(x_{i+1}, x_i) \times (y_{j+1}, y_j) \,|\, i = 0, \ldots, L_1 + 1, j = 0, \ldots, L_2 + 1\}$ where $x_{L_1+1} = 0$, $y_{L_2+1} = 0$, and $x_i = q^i$, $i = 0, \ldots, L_1$, $y_j = q^j$, $j = 0, \ldots, L_2$.

Remark 3.3 We restricted ourselves to quadrilateral mesh patches. However, analogous refinement strategies can also be defined on triangular patches.

3.3. Approximation of Layers on Boundary Layer Meshes

The purpose of the present section is to illustrate that the mesh patches presented above are well-suited for the approximation of layer functions at robust exponential rates. The approximation results presented here cover not only the approximation in "energy norms" but also in stronger norms in order to enable us to analyze the SDFEM below. As the construction of the interpolants is fairly technical, the actual proofs are collected in Appendix A.

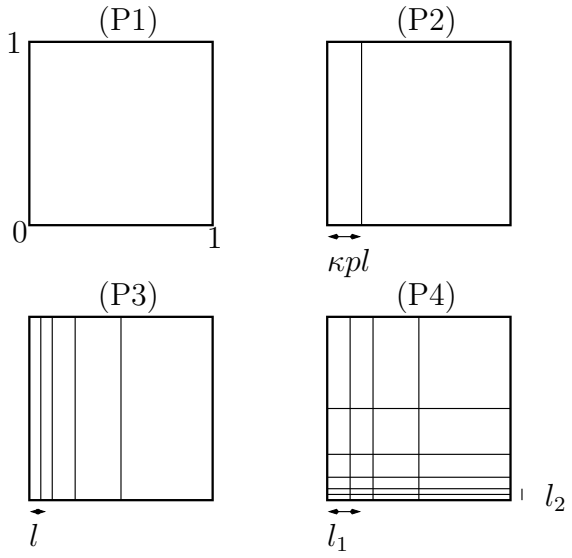

Figure 2: Reference patches (P1)–(P4).

We start at this point by showing that the property of being a function of boundary layer type in the sense of Definition 3.1 is invariant under analytic changes of variables. This will be our tool to be able to restrict our attention to very few reference configurations.
Throughout, let S denote the closed reference square, i.e., $S = [0,1]^2$.

Lemma 3.4 *Let $S = [0,1]^2$ and $F : S \to \mathbb{R}^2$, $(x,y) \mapsto (r,s) = F(x,y)$ be an analytic diffeomorphism in a neighbourhood of S. Assume that $r = r(x,y)$ satisfies $r(0,y) = 0$ (i.e., that F maps the the line $x = 0$ into the line $r = 0$). Let u be of boundary layer type and satisfy (3.2) on $F(S)$. Then there are C', γ', $d' > 0$ depending only on the constants C, γ, d of (3.2) and the mapping F such that the function $\tilde{u} := u \circ F$ satisfies on S:*

$$|\partial_x^m \partial_y^n \tilde{u}(x,y)| \leq C'(\gamma')^{m+n} n! \max\{m, l^{-1}\}^m e^{-d'x/l} \qquad \forall (m,n) \in \mathbb{N}_0^2, \quad (x,y) \in S. \tag{3.5}$$

Proof: The proof is essentially the one presented in Lemma 3.6 of [19]. □

The merit of Lemma 3.4 is that it allows us to perform approximation theory on reference configurations in the framework of the *mesh patches* introduced above. We may therefore assume for the purpose of the present section that a function u of boundary layer type is given on S and satisfies (3.5).
We can now formulate the following three approximation results for functions satisfying (3.5). The proofs are relegated to Appendix A. We start with the two-element patch (P2).

Theorem 3.5 *For $\kappa > 0$, $p \in \mathbb{N}$ let $\overline{x} := \min\{1/2, \kappa pl\}$ and define the "two-element mesh" $\hat{\mathcal{T}}_{\kappa pl} = \{(0,\overline{x}) \times (0,1), (\overline{x},1) \times (0,1)\}$. Let u satisfy (3.5). Then there are C, σ, κ_0 depending only on C, γ, d of (3.5) such that for $\kappa \in (0,\kappa_0)$ there is $\pi_p \in S^p(\hat{\mathcal{T}}_{\kappa pl})$ with*

$$\begin{aligned} \kappa pl \|\nabla(u - \pi_p)\|_{L^2(S)} + \|u - \pi_p\|_{L^2(S)} &\leq C l^{1/2} e^{-\sigma \kappa p}, \\ \kappa pl \|\nabla(u - \pi_p)\|_{L^\infty(S)} + \|u - \pi_p\|_{L^\infty(S)} &\leq C e^{-\sigma \kappa p}. \end{aligned}$$

Remark 3.6 The two-element patch (P2) is essentially the minimal mesh that can resolve functions of layer type at a robust exponential rate; we refer to [24] where necessity of a small element of size $O(pl)$ in the layer was demonstrated for a 1-D model problem.

The next theorem circumvents the need to choose κ by considering meshes that are graded geometrically towards the line $x = 0$. These meshes are the ones presented as type (P3):

Theorem 3.7 *Let u satisfy (3.5) on S. Let $q \in (0,1)$ be a fixed grading factor and let $L \in \mathbb{N}_0$ be such that $q^L \approx l$. Let $\hat{\mathcal{T}}_x$ be a mesh on $(0,1)$ given by the points $x_{L+1} = 0$, $x_i = q^i$ for $i = 0, \ldots, L$. Let $\hat{\mathcal{T}}_y$ be an arbitrary mesh on $(0,1)$ and $\hat{\mathcal{T}} = \hat{\mathcal{T}}_x \times \hat{\mathcal{T}}_y$. Then there are constants C, $\sigma > 0$ depending only on C and γ of (3.5) and an interpolant $\pi_p \in S^p(\hat{\mathcal{T}})$ such that*

$$\begin{aligned} l\|\nabla(u-\pi_p)\|_{L^2(S)} + \|u-\pi_p\|_{L^2(S)} &\leq Cl^{1/2}e^{-\sigma p}, \\ l\|\nabla(u-\pi_p)\|_{L^\infty(S)} + \|u-\pi_p\|_{L^\infty(S)} &\leq Ce^{-\sigma p}, \\ \sum_{K\in\hat{\mathcal{T}}} \frac{h_{K,min}h_{K,max}}{l} l^2\|\nabla(u-\pi_p)\|^2_{L^\infty(K)} &\leq Ce^{-\sigma p}, \\ \sum_{K\in\hat{\mathcal{T}}} h_{K,min}\|\nabla(u-\pi_p)\|^2_{L^2(K)} &\leq Ce^{-\sigma p}. \end{aligned}$$

It should be noted that the number of elements in the meshes considered in Theorem 3.7 is not independent of the length scale l of the layer: From the condition $q^L \approx l$ we immediately get $L = O(|\ln l|)$. Nevertheless, this is a rather weak side condition. The preceding two theorems were concerned with the approximation of a single layer. Let us now turn to the problem of approximating two layers on S located at the lines $x = 0$ and $y = 0$. Specifically, let u_1, u_2 be two functions of boundary layer type satisfying

$$|\partial_x^m \partial_y^n u_1(x,y)| \leq C\gamma^{m+n} n! \max\{l_1^{-1}, m\}^m e^{-dx/l_1} \quad \forall (m,n) \in \mathbb{N}_0^2, \quad (x,y) \in S, \tag{3.6}$$

$$|\partial_y^m \partial_x^n u_2(x,y)| \leq C\gamma^{m+n} n! \max\{l_2^{-1}, m\}^m e^{-dy/l_2} \quad \forall (m,n) \in \mathbb{N}_0^2, \quad (x,y) \in S. \tag{3.7}$$

The simultaneous approximation of these two different layers on the same domain S can be handled by tensor product meshes of the type (P4):

Theorem 3.8 *Let u_1, u_2 satisfy (3.6), (3.7), $q \in (0,1)$ be a fixed grading factor and let L_1, $L_2 \in \mathbb{N}_0$ be such that $q^{L_1} \approx l_1$, $q^{L_2} \approx l_2$. Let $\hat{\mathcal{T}}_1$, $\hat{\mathcal{T}}_2$ be two meshes on $(0,1)$ given by the points*

$$x_{L_1+1} = 0, \quad x_i = q^i, \quad i = 0, \ldots, L_1 \qquad y_{L_2+1} = 0, \quad y_j = q^j, \quad j = 0, \ldots, L_2,$$

respectively, and set $\hat{\mathcal{T}} := \hat{\mathcal{T}}_1 \times \hat{\mathcal{T}}_2$. Then there are constants C, $\sigma > 0$ independent of p, l_1, l_2 and interpolants $\pi_i \in S^p(\hat{\mathcal{T}})$, $i = 1, 2$, such that for $i = 1, 2$ there holds:

$$\begin{aligned} l_i\|\nabla(u_i-\pi_i)\|_{L^2(S)} + \|u_i-\pi_i\|_{L^2(S)} &\leq Cl_i^{1/2}e^{-\sigma p}, \\ l_i\|\nabla(u_i-\pi_i)\|_{L^\infty(S)} + \|u_i-\pi_i\|_{L^\infty(S)} &\leq Ce^{-\sigma p}, \\ \sum_{K\in\hat{\mathcal{T}}} \frac{h_{K,min}h_{K,max}}{l_i} l_i^2\|\nabla(u_i-\pi_i)\|^2_{L^\infty(K)} &\leq Ce^{-\sigma p}, \\ \sum_{K\in\hat{\mathcal{T}}} h_{K,min}\|\nabla(u_i-\pi_i)\|^2_{L^2(K)} &\leq Ce^{-\sigma p}. \end{aligned}$$

Remark 3.9 Our meshes consist of quadrilaterals only. However, similar results hold true on triangular patches as well.

4. Stability of the SDFEM

In this section we address the stability of the SDFEM on boundary layer meshes. This problem is closely related to inverse inequalities on anisotropic elements which are presented in Section 4.1.

4.1. Inverse Inequalities

We recall the basic inverse estimate valid on the reference element $\hat{K}$ ($= \hat{Q}$ or $\hat{T}$) [23]:

Lemma 4.1 *There exists a constant C independent of p such that*

$$\|\nabla \Pi_p\|_{L^2(\hat{K})} \leq C p^2 \|\Pi_p\|_{L^2(\hat{K})}, \qquad \|\Pi_p\|_{L^1(\partial\hat{K})} \leq C p \|\Pi_p\|_{L^2(\hat{K})}$$

for all polynomials $\Pi_p \in \mathcal{S}^p(\hat{K})$.

On a boundary layer mesh $\mathcal{T}$ we have:

Proposition 4.2 *Let K be an element of the boundary layer mesh $\mathcal{T}$ and Π_p a mapped polynomial on K, that is $\Pi_p \circ F_K \in \mathcal{S}^p(\hat{K})$. Then there exists a constant $C_{inv} > 0$ independent of p and of the elements of $\mathcal{T}$ such that*

$$C_{inv} \frac{h_K^2}{p^4} \|\nabla \Pi_p\|^2_{L^2(K)} \leq \|\Pi_p\|^2_{L^2(K)}, \tag{4.1}$$

$$C_{inv} \frac{h_K^2}{p^4} \|D^2 \Pi_p\|^2_{L^2(K)} \leq \|\nabla \Pi_p\|^2_{L^2(K)}, \tag{4.2}$$

$$\frac{C_{inv}}{p^2} \frac{h_{K,min}}{h_{K,max}} \|\Pi_p\|^2_{L^1(\partial K)} \leq \|\Pi_p\|^2_{L^2(K)}. \tag{4.3}$$

Proof: The element mapping $F_K : \hat{K} \to K$ can be factorized into $F_K = \tilde{F}_K \circ F_1$, where F_1 is the change of variables $\xi = h_x \hat{x}$, $\eta = h_y \hat{y}$ from $\hat{K}$ onto $\hat{R}_K$. h_x and h_y are the scaling factors in accordance to Definition 3.2 and (3.4). Taking into account (3.3) we see that

$$\begin{aligned} C^{-1} h_{K,max} &\leq \max\{h_x, h_y\} \leq C h_{K,max}, \\ C^{-1} h_{K,min} &\leq \min\{h_x, h_y\} \leq C h_{K,min}. \end{aligned} \tag{4.4}$$

Fix now a mapped polynomial Π_p on K, i.e., $\Pi_p \circ F_K \in \mathcal{S}^p(\hat{K})$. We set $\tilde{\Pi}_p(\xi, \eta) = \Pi_p \circ \tilde{F}_K(\xi, \eta)$ and $\tilde{\Pi}_p(\hat{x}, \hat{y}) = \Pi_p \circ F_K(\hat{x}, \hat{y})$. Using again (3.3) we have

$$\|\nabla \Pi_p\|_{L^2(K)} \leq C \|\nabla \tilde{\Pi}_p\|_{L^2(\hat{R}_K)}, \qquad \|\tilde{\Pi}_p\|_{L^2(\hat{R}_K)} \leq C \|\Pi_p\|_{L^2(K)}, \tag{4.5}$$

$$\|\nabla \tilde{\Pi}_p\|_{L^2(\hat{R}_K)} \leq C \|\nabla \Pi_p\|_{L^2(K)},$$

$$\|D^2 \Pi_p\|_{L^2(K)} \leq C \|\tilde{\Pi}_p\|_{H^2(\hat{R}_K)}. \tag{4.6}$$

From a Poincaré inequality for convex sets (see, e.g., Section 7.8 of [9]) there holds

$$\inf_{c\in\mathbb{R}} \|\tilde{\Pi}_p - c\|_{L^2(\hat{R}_K)} \leq C\frac{h_x^2+h_y^2}{\sqrt{h_x h_y}}\|\nabla\tilde{\Pi}_p\|_{L^2(\hat{R}_K)}.$$

Thus, observing that the right-hand side of (4.6) does not change if Π_p is replaced with $\Pi_p + c$, $c \in \mathbb{R}$, we obtain

$$\|D^2\Pi_p\|^2_{L^2(K)} \leq C\left[\|D^2\tilde{\Pi}_p\|^2_{L^2(\hat{R}_K)} + \frac{h_x^2+h_y^2}{h_x h_y}\|\nabla\tilde{\Pi}_p\|^2_{L^2(\hat{R}_K)}\right],$$

where we additionally exploited the trivial fact that $h_x^2 + h_y^2$ is bounded. The inverse estimates in Lemma 4.1 and a scaling argument applied to $\tilde{\Pi}_p \circ F_1$ yield

$$\|\frac{\partial\tilde{\Pi}_p}{\partial\xi}\|_{L^2(\hat{R}_K)} \leq Ch_x^{-1}p^2\|\tilde{\Pi}_p\|_{L^2(\hat{R}_K)}, \qquad \|\frac{\partial\tilde{\Pi}_p}{\partial\eta}\|_{L^2(\hat{R}_K)} \leq Ch_y^{-1}p^2\|\tilde{\Pi}_p\|_{L^2(\hat{R}_K)}. \tag{4.7}$$

Combining (4.4), (4.5) and (4.7) results in

$$\begin{aligned}
&\frac{h_{K,max}^2 h_{K,min}^2}{h_{K,max}^2+h_{K,min}^2}\|\nabla\Pi_p\|^2_{L^2(K)} \leq C\frac{h_x^2h_y^2}{h_x^2+h_y^2}\|\nabla\tilde{\Pi}_p\|^2_{L^2(\hat{R}_K)}\\
&= C\frac{h_x^2h_y^2}{h_x^2+h_y^2}\{\|\frac{\partial\tilde{\Pi}_p}{\partial\xi}\|^2_{L^2(\hat{R}_K)} + \|\frac{\partial\tilde{\Pi}_p}{\partial\eta}\|^2_{L^2(\hat{R}_K)}\}\\
&\leq Cp^4\frac{h_y^2+h_x^2}{h_x^2+h_y^2}\|\tilde{\Pi}_p\|^2_{L^2(\hat{R}_K)} \leq Cp^4\|\Pi_p\|^2_{L^2(K)}.
\end{aligned}$$

Analogously,

$$\begin{aligned}
&\frac{h_{K,max}^2 h_{K,min}^2}{h_{K,max}^2+h_{K,min}^2}\|D^2\Pi_p\|^2_{L^2(K)} \leq C\frac{h_x^2h_y^2}{h_x^2+h_y^2}\|D^2\tilde{\Pi}_p\|^2_{L^2(\hat{R}_K)} + C\|\nabla\tilde{\Pi}_p\|_{L^2(\hat{R})}\\
&\leq C\frac{h_x^2h_y^2}{h_x^2+h_y^2}\{\|\tilde{\Pi}_{p,\xi\xi}\|^2_{L^2(\hat{R}_K)} + 2\|\tilde{\Pi}_{p,\xi\eta}\|^2_{L^2(\hat{R}_K)} + \|\tilde{\Pi}_{p,\eta\eta}\|^2_{L^2(\hat{R}_K)}\} + C\|\nabla\tilde{\Pi}_p\|_{L^2(\hat{R})}\\
&\leq C\frac{p^4}{h_x^2+h_y^2}\{h_y^2\|\tilde{\Pi}_{p,\xi}\|^2_{L^2(\hat{R}_K)} + h_x^2\|\tilde{\Pi}_{p,\xi}\|^2_{L^2(\hat{R}_K)} + h_x^2\|\tilde{\Pi}_{p,\eta}\|^2_{L^2(\hat{R}_K)}\} + C\|\nabla\tilde{\Pi}_p\|_{L^2(\hat{R})}\\
&\leq C\frac{h_y^2+h_x^2}{h_x^2+h_y^2}p^4\|\nabla\tilde{\Pi}_p\|^2_{L^2(\hat{R}_K)} \leq Cp^4\|\nabla\Pi_p\|^2_{L^2(K)}.
\end{aligned}$$

This shows (4.1) and (4.2).
To prove (4.3), we calculate similarly:

$$\begin{aligned}
\|\Pi_p\|_{L^1(\partial K)} &\leq C\|\tilde{\Pi}_p\|_{L^1(\partial R_K)} \leq Ch_{K,max}\|\hat{\Pi}_p\|_{L^1(\partial\hat{K})},\\
\|\hat{\Pi}_p\|_{L^2(\hat{K})} &= \sqrt{\frac{1}{h_{K,max}h_{K,min}}}\|\tilde{\Pi}_p\|_{L^2(R_K)} \leq C\sqrt{\frac{1}{h_{K,max}h_{K,min}}}\|\Pi_p\|_{L^2(K)}.
\end{aligned}$$

(4.3) can now be inferred from these last two estimates together with Lemma 4.1. □

4.2. Stability in the SDFEM Norm

Let $\mathcal{T}$ be a boundary layer mesh. We show that the bilinear form B_{SD} of the SDFEM is coercive on $S_0^p(\mathcal{T}) \times S_0^p(\mathcal{T})$.

Proposition 4.3 *Let the weights ρ_K be given by*

$$\begin{aligned} \rho_K &= \frac{h_K}{p_K} \qquad \text{if } p_K^7 h_K^{-3} \varepsilon^2 \leq C \text{ for some constant } C > 0, \\ \rho_K &= \frac{h_K}{p_K^2} \qquad \text{else.} \end{aligned} \tag{4.8}$$

Then there exists a constant δ_0 just depending on C_{inv} in Lemma 4.2, the constant C of (4.8), and on the data $\vec{a}$, b such that for parameters δ_K satisfying $0 \leq \delta_K \leq \delta_0$ the SDFEM (2.7) is coercive, i.e.

$$\frac{1}{2}\|U\|_{SD}^2 \leq B_{SD}(U,U) \qquad \forall U \in S_0^p(\mathcal{T}).$$

Proof: Assume first that $0 \leq \delta_K \leq \delta_0'$ with δ_0' to be chosen later on. We have

$$B_{SD}(U,U) = B(U,U) + \sum_{K \in \mathcal{T}} \delta_K \rho_K \int_K (-\varepsilon \Delta U + \vec{a} \cdot \nabla U + bU)(\vec{a} \cdot \nabla U) dx.$$

Due to assumption (2.3) we have $B(U,U) \geq \|U\|_E^2$ and it remains to estimate the critical terms

$$\begin{aligned} A_1 &:= \sum_{K \in \mathcal{T}} A_{1,K} := \sum_{K \in \mathcal{T}} \delta_K \rho_K \int_K -\varepsilon \Delta U (\vec{a} \cdot \nabla U) dx, \\ A_2 &:= \sum_{K \in \mathcal{T}} \delta_K \rho_K \int_K bU (\vec{a} \cdot \nabla U) dx. \end{aligned}$$

We first bound A_1: Fix $K \in \mathcal{T}$ and consider the case where $\rho_K = \frac{h_K}{p_K^2}$. We use Cauchy-Schwarz and the inverse estimates in Proposition 4.2 to get

$$\begin{aligned} |A_{1,K}| &\leq \delta_K \rho_K \varepsilon \|\Delta U\|_{L^2(K)} \|\vec{a} \cdot \nabla U\|_{L^2(K)} \\ &\leq C \delta_K \rho_K \frac{p_K^2}{h_K} \varepsilon \|\nabla U\|_{L^2(K)}^2 \leq C \delta_0' \varepsilon \|\nabla U\|_{L^2(K)}^2. \end{aligned}$$

If $\rho_K = \frac{h_K}{p_K}$, we use (4.8) and get by a twofold application of Proposition 4.2:

$$\begin{aligned} |A_{1,K}| &\leq \delta_K \rho_K \varepsilon^2 \|\Delta U\|_{L^2(K)}^2 + \frac{1}{4} \delta_K \rho_K \|\vec{a} \cdot \nabla U\|_{L^2(K)}^2 \\ &\leq C \delta_0' \rho_K \varepsilon^2 \frac{p_K^8}{h_K^4} \mu \|U\|_{L^2(K)}^2 + \frac{1}{4} \delta_K \rho_K \|\vec{a} \cdot \nabla U\|_{L^2(K)}^2 \\ &\leq C \delta_0' \mu \|U\|_{L^2(K)}^2 + \frac{1}{4} \delta_K \rho_K \|\vec{a} \cdot \nabla U\|_{L^2(K)}^2. \end{aligned}$$

Hence, we get for A_1 the bound

$$|A_1| \leq C \delta_0' \|U\|_E^2 + \frac{1}{4} \sum_{K \in \mathcal{T}} \delta_K \rho_K \|\vec{a} \cdot \nabla U\|_{L^2(K)}^2.$$

The second term A_2 is estimated as follows:

$$\begin{aligned}
|A_2| &\leq C \sum_{K\in\mathcal{T}} \delta_K \rho_K \|U\|_{L^2(K)} \|\vec{a}\cdot\nabla U\|_{L^2(K)} \\
&\leq C \sum_{K\in\mathcal{T}} \sqrt{\delta_K\rho_K}\|U\|_{L^2(K)} \sqrt{\delta_K\rho_K}\|\vec{a}\cdot\nabla U\|_{L^2(K)} \\
&\leq C \sum_{K\in\mathcal{T}} \delta_K \rho_K \|U\|^2_{L^2(K)} + \frac{1}{4}\sum_{K\in\mathcal{T}} \delta_K\rho_K \|\vec{a}\cdot\nabla U\|^2_{L^2(K)} \\
&\leq C\delta_0'\mu\|U\|^2_{L^2(\Omega)} + \frac{1}{4}\sum_{K\in\mathcal{T}} \delta_K\rho_K \|\vec{a}\cdot\nabla U\|^2_{L^2(K)}.
\end{aligned}$$

Combining the above estimates gives

$$B_{SD}(U,U) \geq (1 - C\delta_0')\|U\|_E^2 + \frac{1}{2}\sum_{K\in\mathcal{T}} \delta_K\rho_K\|\vec{a}\cdot\nabla U\|^2_{L^2(K)}.$$

Selecting now $\delta_0' \leq \delta_0 := \frac{1}{2C}$ finishes the proof. □

Remark 4.4 In Proposition 4.3 we chose $\rho_K = h_K/p_K$ when ε is small compared with h_K and $1/p_K$ in the sense of (4.8). This particular choice is motivated by our analysis on quasiuniform meshes in Remark 5.9 to give optimal *hp*-error bounds. By similar techniques stability of the SDFEM can also be obtained for $\rho_K = h_K/p_K^\alpha$ for $\alpha \geq 0$ when a condition analogous to (4.8) is satisfied. The performance of the SDFEM in dependence on α is investigated numerically in Section 6.

5. Consistency of the SDFEM

In this section the *hp*-approximation results of Section 3 and the stability properties in Section 4 are combined into our main result: We prove in Section 5.1, 5.2 and 5.3 that exponential rates of convergence can be achieved in the *hp*-SDFEM provided that all layer components present in the solutions are resolved. Moreover, in Section 5.4 we derive optimal *hp* convergence results on shape regular meshes valid for smooth solutions.

5.1. Exponential Convergence

By Proposition 4.3 we may assume that the SDFEM is coercive on $S_0^p(\mathcal{T}) \times S_0^p(\mathcal{T})$, i.e., there holds for some $c_0 > 0$

$$c_0\|U\|^2_{SD} \leq B_{SD}(U,U) \qquad \forall U \in S_0^p(\mathcal{T}).$$

We use the Galerkin orthogonality in (2.10) and obtain for every interpolant $Iu \in S_0^p(\mathcal{T})$

$$\begin{aligned}
& c_0\|U - Iu\|^2_{SD} \leq B_{SD}(u - Iu, U - Iu) \\
= \;& \varepsilon\int_\Omega \nabla(u-Iu)\nabla(U-Iu)dx + \int_\Omega (\vec{a}\cdot\nabla(u-Iu) + b(u-Iu))(U-Iu)dx \\
& + \sum_{K\in\mathcal{T}} \delta_K\rho_K \int_K (-\varepsilon\Delta(u-Iu) + \vec{a}\cdot\nabla(u-Iu) + b(u-Iu))(\vec{a}\cdot\nabla(U-Iu))dx \\
=: \;& S_1(\eta, U-Iu) + S_2(\eta, U-Iu) + S_3(\eta, U-Iu),
\end{aligned}$$

where we wrote $\eta = u - Iu$. Next, we introduce the semi-norms

$$T_i(\eta) := \sup_{0 \neq \pi \in S_0^p(\mathcal{T})} \frac{S_i(\eta, \pi)}{\|\pi\|_{SD}}, \qquad i \in \{1, 2, 3\} \tag{5.1}$$

and then get

$$\|u - U\|_E \leq \|u - Iu\|_E + \|U - Iu\|_{SD} \leq \|\eta\|_E + c_0^{-1} \left[T_1(\eta) + T_2(\eta) + T_3(\eta)\right]. \tag{5.2}$$

Note that the interpolant $Iu \in S_0^p(\mathcal{T})$ was so far not specified and is still at our disposal. Let us write $Iu \in S_0^p(\mathcal{T})$ in the form $Iu = Iu_{smooth} + Iu_{layer} + Iu_{rem}$ and introduce $\eta_{smooth} = u_{smooth} - Iu_{smooth}$, $\eta_{layer} = u_{layer} - Iu_{layer}$, $\eta_{rem} = u_{rem} - Iu_{rem}$. As the expressions T_i are semi-norms on $H^1(\Omega)$, we get the *a priori* bound

$$\begin{aligned} \|U - Iu\|_{SD} \leq{}& \|\eta_{smooth}\|_E + \|\eta_{layer}\|_E + \|\eta_{rem}\|_E \\ &+ c_0^{-1} \Big(\sum_{i=1}^{3} T_i(\eta_{smooth}) + T_i(\eta_{layer}) + T_i(\eta_{rem})\Big). \end{aligned} \tag{5.3}$$

The smooth component u_{smooth} and the layer component u_{layer} are (piecewise) analytic and they can be approximated at robust exponential rates of convergence using, for example, the mesh patches introduced in Section 3.2. This approximability result holds for the SDFEM as well. As no regularity theory is available for the remainder u_{rem} we will restrict ourselves to the assumption that u_{rem} vanishes (or at least is negligible). In this context, we can formulate the following main result of this paper:

Theorem 5.1 *Let u be the solution of (2.1), (2.2). Assume that u is of the form $u = u_{smooth} + u_{layer}$ with u_{smooth} being (piecewise) analytic and u_{layer} consisting of finitely many layer components in the sense of Definition 3.1. Let $U \in S_0^p(\mathcal{T})$ be the SDFEM solution where we assume that the method is stable according to Proposition 4.3 and satisfies (2.11), (2.13). Let $\mathcal{T}$ be a boundary layer mesh on Ω generated by mesh patches of the form (P1), (P3), or (P4) such that all layer components can be resolved. Then there are C, $\sigma > 0$ such that for the error $u - U$ there holds*

$$\|u - U\|_E \leq C|\mathcal{T}|^{1/2} e^{-\sigma p},$$

where $|\mathcal{T}|$ stands for the number of elements in the triangulation $\mathcal{T}$.

Remark 5.2 We excluded the use of the "two-element" patch in Theorem 5.1 as we wanted to be able to handle the case of the simultaneous approximation of two different layers on the same patch. The mesh patches of type (P2) can be used if only one type of layer has to be approximated on each patch. A careful inspection of the proof of Proposition 5.7 shows that the factor $|\mathcal{T}|^{1/2}$ stems from the approximation of *parabolic* layers on meshes of type (P3) and (P4). Hence, the factor $|\mathcal{T}|^{1/2}$ could be avoided if only exponential layers occur. If mesh patches of type (P3) or (P4) are used in the generation of the mesh, then the number of elements (and hence also the number of degrees of freedom) does depend weakly on ε, i.e. $|\mathcal{T}| \leq C(\ln \varepsilon)^2$ and $\text{DOF} \leq Cp^2(\ln \varepsilon)^2$.

Section 5.2 and Section 5.3 are devoted to the proof of Theorem 5.1, i.e., to obtaining bounds for the terms $T_i(\eta_{smooth})$ and $T_i(\eta_{layer})$ in (5.3). The proof of Theorem 5.1 will then follow from (5.3), the fact that the macro element maps are analytic diffeomorphism and from Propositions 5.4, 5.7 ahead. Strictly speaking, one has to check that the patchwise defined interpolants of these propositions lead to an element of $S_0^p(\mathcal{T})$; this is indeed the case.

5.2. hp-Approximation of the Smooth Part

For the smooth part u_{smooth} we have the following lemma (cf., e.g., [22]):

Lemma 5.3 *Let $\mathcal{T}$ be an arbitrary boundary layer mesh in the sense of Definition 3.2 and let $\eta \in H_0^1(\Omega) \cap \Pi_{K\in\mathcal{T}} H^2(K)$. Then there is $C > 0$ depending only on Ω and the coefficient functions $\vec{a}$, b such that*

$$\begin{aligned}
|T_1(\eta)| &\leq \varepsilon^{1/2} \left(\sum_{K\in\mathcal{T}} \|\eta\|^2_{H^1(K)} \right)^{1/2}, \\
|T_2(\eta)| &\leq C \min \left\{ \|\eta\|_{H^1(\Omega)}, \left(\sum_{K\in\mathcal{T}} \frac{1}{\varepsilon + \delta_K \rho_K} \|\eta\|^2_{L^2(K)} \right)^{1/2} \right\}, \\
|T_3(\eta)| &\leq C(\sum_{K\in\mathcal{T}} \delta_K \rho_K \{ \varepsilon^2 \|\eta\|^2_{H^2(K)} + \|\eta\|^2_{H^1(K)} + \|\eta\|^2_{L^2(K)} \})^{\frac{1}{2}}.
\end{aligned}$$

Proof: The bounds for $T_1(\eta)$ and $T_3(\eta)$ are obvious. To estimate $T_2(\eta)$, let $\pi \in S_0^p(\mathcal{T})$ and integrate the expression $S_2(\eta, \pi)$ in (5.1) by parts to get

$$\int_\Omega (\vec{a} \cdot \nabla \eta) \pi \, dx = - \int_\Omega \eta \vec{a} \cdot \nabla \pi \, dx - \int_\Omega (\operatorname{div} \vec{a}) \eta \pi \, dx.$$

Hence, we have

$$\left| \int_\Omega \vec{a} \cdot \nabla \eta \pi \, dx \right| \leq \sum_{K\in\mathcal{T}} \|\eta\|_{L^2(K)} \|\vec{a} \cdot \nabla \pi\|_{L^2(K)} + C \|\eta\|_{L^2(\Omega)} \|\pi\|_{L^2(\Omega)}.$$

As by the choice of the parameters ε, $\delta_K \rho_K$ there holds $\varepsilon + \delta_K \rho_K \leq C$ for some $C > 0$, we can estimate

$$\|\eta\|_{L^2(\Omega)} \|\pi\|_{L^2(\Omega)} \leq C \left\{ \sum_{K\in\mathcal{T}} \frac{1}{\varepsilon + \delta_K \rho_K} \|\eta\|^2_{L^2(K)} \right\}^{1/2} \|\pi\|_{SD}.$$

Next, the Cauchy-Schwarz inequality for sums gives

$$\begin{aligned}
&\sum_{K\in\mathcal{T}} \|\eta\|_{L^2(K)} \|\vec{a} \cdot \nabla \pi\|_{L^2(K)} \\
&\quad \leq \left\{ \sum_{K\in\mathcal{T}} \frac{1}{\varepsilon + \delta_K \rho_K} \|\eta\|^2_{L^2(K)} \right\}^{1/2} \left\{ \sum_{K\in\mathcal{T}} (\varepsilon + \delta_K \rho_K) \|\vec{a} \cdot \nabla \pi\|^2_{L^2(K)} \right\}^{1/2} \\
&\quad \leq C \left\{ \sum_{K\in\mathcal{T}} \frac{1}{\varepsilon + \delta_K \rho_K} \|\eta\|^2_{L^2(K)} \right\}^{1/2} \|\pi\|_{SD}
\end{aligned}$$

The desired bounds for $T_2(\eta)$ now follow. □

For the smooth part u_{smooth}, we can now formulate:

Proposition 5.4 *Let $\mathcal{T}$ be boundary layer mesh in the sense of Definition 3.2 consisting of quadrilaterals only. Assume that (2.11) and (2.13) hold. Let u_{smooth} be analytic on $\overline{\Omega}$. Let $Iu_{smooth} \in S^p(\mathcal{T})$ be the piecewise Gauss-Lobatto interpolant of u_{smooth}. Then there are C, $\sigma > 0$ such that, upon writing $\eta_{smooth} = u_{smooth} - Iu_{smooth}$, there holds*

$$\|\eta_{smooth}\|_E + \sum_{i=1}^{3} |T_i(\eta_{smooth})| \leq Ce^{-\sigma p}.$$

Proof: The proof follows directly from the observation that for each element K there holds $\|\eta_{smooth}\|_{W^{2,\infty}(K)} \leq Ce^{-\sigma p}$. □

5.3. hp-Approximation of the Layer Part

For the approximation of exponential boundary layers, Lemma 5.3 is not appropriate as it cannot lead to robust estimates. For estimates of the layer part, we have to treat the term T_3 differently. This is accomplished in the next lemma.

Lemma 5.5 *Let $\mathcal{T}$ be an arbitrary boundary layer mesh in the sense of Definition 3.2 and let $\eta \in W^{1,\infty}(\Omega)$. Then there is $C > 0$ depending only on Ω and the coefficient functions $\vec{a}$, b such that*

$$\begin{aligned}
|T_1(\eta)| &\leq \varepsilon^{1/2} \left(\sum_{K\in\mathcal{T}} \|\eta\|^2_{H^1(K)} \right)^{1/2}, \\
|T_2(\eta)| &\leq C \left(\sum_{K\in\mathcal{T}} \frac{1}{\varepsilon + \delta_K \rho_K} \|\eta\|^2_{L^2(K)} \right)^{1/2}, \\
|T_3(\eta)| &\leq C \left[E_1(\eta) + E_2(\eta) + E_3(\eta) + \|\eta\|_{L^2(\Omega)} \right]
\end{aligned}$$

where

$$E_1(\eta) := \left\{ \sum_{K\in\mathcal{T}} (\delta_K \rho_K)^2 \frac{p^4}{p^4\varepsilon + h^2_{K,min}} \frac{p^4\varepsilon}{h^2_{K,min}} \left[\varepsilon \|\nabla\eta\|^2_{L^2(K)} \right] \right\}^{1/2}, \tag{5.4}$$

$$E_2(\eta) := \left\{ \sum_{K\in\mathcal{T}} (\delta_K \rho_K)^2 \frac{p^4}{p^4\varepsilon + h^2_{K,min}} \frac{p^2 h_{K,max}}{h_{K,min}} \left[\varepsilon^2 \|\nabla\eta\|^2_{L^\infty(K)} \right] \right\}^{1/2}, \tag{5.5}$$

$$E_3(\eta) := \left\{ \sum_{K\in\mathcal{T}} \min\left\{ F_{1,K}(\eta), F_{2,K}(\eta) \right\} \right\}^{1/2}, \tag{5.6}$$

$$F_{1,K}(\eta) := (\delta_K \rho_K)^2 \frac{p^4}{p^4\varepsilon + h^2_{K,min}} \left[\frac{p^4}{h^2_{K,min}} \|\eta\|^2_{L^2(K)} + \frac{p^2 h_{K,max}}{h_{K,min}} \|\eta\|^2_{L^\infty(K)} \right], \tag{5.7}$$

$$F_{2,K}(\eta) := \delta_K \rho_K \|\vec{a} \cdot \nabla\eta\|^2_{L^2(K)}. \tag{5.8}$$

Remark 5.6 On polygons, the exact solution u has corner singularities such that estimates that contain terms like $\|\nabla\eta\|_{L^\infty(K)}$ are not directly applicable. However, the proof of Lemma 5.5 shows that these L^∞ bounds are not necessary in all elements. Nevertheless, to get meaningful bounds avoiding these L^∞ estimates, more information about the regularity of the exact solution in the vicinity of the corners is necessary. Such regularity issues must be addressed in future work.

Proof of Lemma 5.5 : The bounds on the terms T_1 and T_2 are those of Lemma 5.3. We can therefore turn directly to bounding $T_3(\eta)$. For any $\pi \in S_0^p(\mathcal{T})$, the term $S_3(\eta,\pi)$ is a sum of integrals over elements K. Each term of this sum can be written as $\delta_K\rho_K(t_1(K) + t_2(K) + t_3(K))$ with

$$t_1(K) = -\varepsilon\int_K \Delta\eta\,\vec{a}\cdot\nabla\pi\,dx, \qquad t_2(K) = \int_K (\vec{a}\cdot\nabla\eta)\,(\vec{a}\cdot\nabla\pi)\,dx, \qquad t_3(K) = \int_K b\eta\,\vec{a}\cdot\nabla\pi\,dx.$$

To estimate $t_1(K)$, $t_2(K)$, $t_3(K)$, we use that any $\pi \in S_0^p(\mathcal{T})$ satisfies for some $C > 0$

$$\|\pi\|_{H^1(K)} \leq C\sqrt{\frac{p^4}{p^4\varepsilon + h_{K,min}^2}}\|\pi\|_{1,\varepsilon,K}, \tag{5.9}$$

$$\|\pi\|_{H^2(K)} \leq C\frac{p^2}{h_{K,min}}\sqrt{\frac{p^4}{p^4\varepsilon + h_{K,min}^2}}\|\pi\|_{1,\varepsilon,K}, \tag{5.10}$$

where we wrote $\|\pi\|_{1,\varepsilon,K}^2 := \varepsilon\|\nabla\pi\|_{L^2(K)}^2 + \|\pi\|_{L^2(K)}^2$. The estimate for $\|\pi\|_{H^2(K)}$ follows immediately from that for $\|\pi\|_{H^1(K)}$ by Proposition 4.2. For the latter one, we use

$$\|\nabla\pi\|_{L^2(K)} \leq \varepsilon^{-1/2}\left(\varepsilon^{1/2}\|\nabla\pi\|_{L^2(K)}\right), \qquad \|\nabla\pi\|_{L^2(K)} \leq C\frac{p^2}{h_{K,min}}\|\pi\|_{L^2(K)}$$

and thus arrive at

$$\begin{aligned}\|\nabla\pi\|_{L^2(K)}^2 &\leq C\left(\min\{\varepsilon^{-1/2}, p^2h_{K,min}^{-1}\}\right)^2\left[\varepsilon\|\nabla\pi\|_{L^2(K)}^2 + \|\pi\|_{L^2(K)}^2\right]\\ &\leq C\frac{p^4}{\varepsilon + h_{K,min}^2}\|\pi\|_{1,\varepsilon,K}^2.\end{aligned}$$

We estimate now $t_i(K)$ and start with $t_1(K)$: An integration by parts yields

$$t_1(K) = \varepsilon\int_{\partial K}\partial_n\eta\,(\vec{a}\cdot\nabla\pi) - \varepsilon\int_K \nabla\eta\cdot\nabla\pi\mathrm{div}\vec{a}\,dx - \varepsilon\int_K \nabla\eta\cdot(\vec{a}D^2\pi)\,dx,$$

where $D^2\pi$ here stands for the Hessian of π. Each of these three terms is now estimated separately. The first term can be bounded by

$$\begin{aligned}\left|\varepsilon\int_{\partial K}\partial_n\eta\,(\vec{a}\cdot\nabla\pi)\right| &\leq C\varepsilon\|\nabla\eta\|_{L^\infty(K)}\|\nabla\pi\|_{L^1(\partial K)} \leq Cp\sqrt{\frac{h_{K,max}}{h_{K,min}}}\varepsilon\|\nabla\eta\|_{L^\infty(K)}\|\nabla\pi\|_{L^2(K)}\\ &\leq Cp\sqrt{\frac{h_{K,max}}{h_{K,min}}}\sqrt{\frac{p^4}{p^4\varepsilon + h_{K,min}^2}}\varepsilon\|\nabla\eta\|_{L^\infty(K)}\|\pi\|_{1,\varepsilon,K},\end{aligned}$$

using Proposition 4.2 and (5.9). For the remaining two components of t_1 we have

$$\begin{aligned}
\left|\varepsilon \int_K \nabla\eta \cdot \nabla\pi \operatorname{div} \vec{a}\, dx\right| &\leq C\varepsilon \|\nabla\eta\|_{L^2(K)} \|\nabla\pi\|_{L^2(K)} \\
&\leq C\sqrt{\frac{p^4}{\varepsilon p^4 + h_{K,min}^2}}\varepsilon \|\nabla\eta\|_{L^2(K)} \|\nabla\pi\|_{1,\varepsilon,K}, \\
\left|\varepsilon \int_K \nabla\eta\vec{a} \cdot D^2\pi\, dx\right| &\leq C\varepsilon \|\nabla\eta\|_{L^2(K)} \|\pi\|_{H^2(K)} \\
&\leq C\frac{p^2}{h_{K,min}}\sqrt{\frac{p^4}{p^4\varepsilon + h_{K,min}^2}}\varepsilon \|\nabla\eta\|_{L^2(K)} \|\pi\|_{1,\varepsilon,K}.
\end{aligned}$$

Therefore, we get for $t_1(K)$:

$$|t_1(K)| \leq C\sqrt{\frac{p^4}{p^4\varepsilon + h_{K,min}^2}} \left[\varepsilon^{1/2}\frac{p^2}{h_{K,min}}\varepsilon^{1/2}\|\nabla\eta\|_{L^2(K)} + p\sqrt{\frac{h_{K,max}}{h_{K,min}}}\varepsilon\|\nabla\eta\|_{L^\infty(K)}\right] \|\pi\|_{1,\varepsilon,K}.$$

The Cauchy-Schwarz inequality for sums now gives

$$\sum_{K\in\mathcal{T}} \delta_K \rho_K |t_1(K)| \leq C\left[E_1(\eta) + E_2(\eta)\right] \|\pi\|_{SD}.$$

We now turn to $t_2(K)$. We have

$$|t_2(K)| = \left|\int_K \vec{a}\cdot\nabla\eta\vec{a}\cdot\nabla\pi\right| \leq \|\vec{a}\cdot\nabla\eta\|_{L^2(K)} \cdot \|\vec{a}\cdot\nabla\pi\|_{L^2(K)}$$

and this gives immediately the term $F_{2,K}(\eta)$ in the minimum occuring in $E_3(\eta)$. We therefore have to see that $t_2(K)$ can also be bounded by $F_{1,K}(\eta)$. To that end, we start just as in the treatment of $t_1(K)$ by an integration by parts to arrive at

$$t_2(K) = \int_{\partial K} \eta(\vec{a}\cdot\nabla\pi)(\vec{a}\cdot\vec{n})\, ds - \int_K \eta(\vec{a}\cdot\nabla\pi)\operatorname{div}\vec{a}\, dx - \int_K \eta\vec{a}\cdot\nabla(\vec{a}\cdot\nabla\pi)\, dx.$$

Proceeding along the same lines as above, we get

$$\begin{aligned}
\left|\int_{\partial K} \eta(\vec{a}\cdot\nabla\pi)(\vec{a}\cdot\vec{n})\, ds\right| &\leq Cp\sqrt{\frac{h_{K,max}}{h_{K,min}}}\sqrt{\frac{p^4}{p^4\varepsilon + h_{K,min}^2}}\|\eta\|_{L^\infty(K)}\|\pi\|_{1,\varepsilon,K}, \\
\left|\int_K \eta(\vec{a}\cdot\nabla\pi)\operatorname{div}\vec{a}\, dx\right| &\leq C\|\eta\|_{L^2(K)}\|\vec{a}\cdot\nabla\pi\|_{L^2(K)} \leq C\|\eta\|_{L^2(K)}\|\pi\|_{H^1(K)} \\
&\leq C\|\eta\|_{L^2(K)}\sqrt{\frac{p^4}{p^4\varepsilon + h_{K,min}^2}}\|\pi\|_{1,\varepsilon,K}, \\
\left|\int_K \eta(\vec{a}\cdot\nabla(\vec{a}\cdot\nabla\pi))\operatorname{div}\vec{a}\, dx\right| &\leq C\|\eta\|_{L^2(K)}\|\pi\|_{H^2(K)} \\
&\leq C\|\eta\|_{L^2(K)}\frac{p^2}{h_{K,min}}\sqrt{\frac{p^4}{p^4\varepsilon + h_{K,min}^2}}\|\pi\|_{1,\varepsilon,K}.
\end{aligned}$$

Therefore,

$$|t_2(K)| \leq C\sqrt{\frac{p^4}{p^4\varepsilon + h_{K,min}^2}}\left[\frac{p^2}{h_{K,min}}\|\eta\|_{L^2(K)} + p\sqrt{\frac{h_{K,max}}{h_{K,min}}}\|\eta\|_{L^\infty(K)}\right]\|\pi\|_{1,\varepsilon,K}.$$

We recognize that this bound leads directly to $F_{1,K}(\eta)$. Finally, bounding

$$|t_3(K)| \leq \|b\|_{L^\infty(\Omega)}\|\eta\|_{L^2(\Omega)}\|\pi\|_{L^2(\Omega)}$$

finishes the proof of the assertions. □

The terms $T_i(\eta_{layer})$ are exponentially small for meshes that do resolve localized small scale features:

Proposition 5.7 *Let $\Omega = \hat{K}$ and let u be a function of boundary layer type defined on $\hat{K}$ satisfying (3.5) for $l = \varepsilon$ or $l = \varepsilon^{1/2}$. Assume that the SDFEM parameters $\{\rho_K\}$ satisfy (2.11) and the non-degeneracy condition (2.13). Let $\hat{\mathcal{T}}$ be one of the patches of type (P2), (P3), or (P4) (in case of (P4) the number of layers in the y-direction is arbitrary). Then there is $\pi \in S^p(\mathcal{T})$ such that the error $\eta := u - \pi$ satisfies on $\hat{K}$ for some C, $\sigma > 0$ independent of p and l*

$$\|\eta\|_E + \sum_{i=1}^{3}|T_i(\eta)| \leq C|\hat{\mathcal{T}}|^{1/2}e^{-\sigma p}.$$

$|\hat{\mathcal{T}}|$ denotes the number of elements of $\hat{\mathcal{T}}$.

Proof: Theorems 3.5, 3.7, 3.8 immediately give that for all patches of type (P2)–(P4) that can resolve the layer there holds

$$\|\eta\|_E \leq Ce^{-\sigma p}, \qquad \varepsilon^{1/2}\|\eta\|_{H^1(\hat{K})} \leq l^{1/2}\|\eta\|_{H^1(\hat{K})} \leq Ce^{-\sigma p}.$$

In order to estimate $T_2(\eta)$, we observe that

$$\frac{1}{\varepsilon + \delta_K\rho_K}\|\eta\|_{L^2(K)}^2 \leq C\frac{1}{\varepsilon + \underline{\delta}h_{K,min}p^{-\alpha}}h_{K,min}h_{K,max}\|\eta\|_{L^\infty(K)}^2 \leq Ce^{-\sigma p}$$

for some appropriate constants C, $\sigma > 0$. Hence,

$$\sum_{K\in\hat{\mathcal{T}}}\frac{1}{\varepsilon + \delta_K\rho_K}\|\eta\|_{L^2(K)}^2 \leq |\hat{\mathcal{T}}|e^{-\sigma p}.$$

It remains to bound $T_3(\eta)$. To that end, we have to estimate E_1, E_2, E_3, and $\|\eta\|_{L^2(\Omega)}$ of Lemma 5.5. The reader may easily convince himself that $E_1(\eta)$ and $E_2(\eta)$ satisfy the desired bounds (even with constants independent of the number of elements of $\hat{\mathcal{T}}$). For bounds on $E_3(\eta)$, we see that for the cases (P3) and (P4) Theorems 3.7 and 3.8 yields immediately the desired bound via

$$E_3^2(\eta) \leq \sum_{K\in\hat{\mathcal{T}}}F_{2,K}(\eta) \leq Ce^{-\sigma p}.$$

For the two-element patch (P2) we see that we can bound

$$\begin{array}{lll} F_{1,K} & \leq & Ce^{-\sigma p} \qquad\qquad\qquad\quad \text{if } h_{K,min} \sim h_{K,max}, \\ F_{2,K} & \leq & C\kappa pl\|\eta\|_{H^1(K)}^2 \leq Ce^{-\sigma p} \quad \text{if } h_{K,min} = \kappa pl. \end{array}$$

This concludes the argument. □

5.4. hp-Approximation on Shape Regular and Quasiuniform Meshes for Smooth Solutions

As a consequence of Lemma 5.3, we derive in this section optimal convergence results in h and p on shape regular meshes. To do so, we assume throughout the section that the condition (4.8) is satisfied and the weights ρ_K are chosen to be h_K/p_K on all elements.
Let $\mathcal{T}$ be a shape regular mesh on Ω and let the solution u of (2.1), (2.2) be in $H^s(\Omega)\cap H_0^1(\Omega)$ for some $s \geq 2$. Particularly, we assume that $u_{smooth} = u$, $u_{layer} = u_{rem} = 0$. U is the SDFEM solution in $S_0^p(\mathcal{T})$. We denote by Iu a suitable hp-interpolant of u in $S_0^p(\mathcal{T})$ which will be specified in (5.12) ahead. From (5.3) and Lemma 5.3 we see that $\|U - Iu\|_{SD}$ can be bounded by

$$C(\sum_{K\in\mathcal{T}}(\varepsilon+\delta_K\rho_K)\|\eta\|^2_{H^1(K)} + \delta_K\rho_K\varepsilon^2\|\eta\|^2_{H^2(K)} + (\delta_K\rho_K + 1 + \frac{1}{\varepsilon+\delta_K\rho_K})\|\eta\|^2_{L^2(K)})^{\frac{1}{2}}. \quad (5.11)$$

We can now choose the interpolant $Iu \in S_0^p(\mathcal{T})$ in such a way that the following hp-approximation properties hold [23]:

$$\|u - Iu\|_{H^r(K)} \leq C\frac{h_K^{\nu_K - r}}{p_K^{s-r}}\|u\|_{H^s(K)}, \qquad 0 \leq r \leq p_K,\ \nu_K = \min(p_K + 1, s). \quad (5.12)$$

Inserting this into the bound (5.11) we get

$$\|U - Iu\|^2_{SD} \leq C\sum_{K\in\mathcal{T}} a_K \frac{h_K^{2\nu_K-2}}{p_K^{2s-2}}\|u\|^2_{H^s(K)} \quad (5.13)$$

with

$$a_K = \{(\varepsilon+\delta_K\rho_K) + \delta_K\rho_K\varepsilon^2\frac{p_K^2}{h_K^2} + (\delta_K\rho_K + 1 + \frac{1}{\varepsilon+\delta_K\rho_K})\frac{h_K^2}{p_K^2}\}. \quad (5.14)$$

Proposition 5.8 *Let $\mathcal{T}$ be a shape regular mesh on Ω and $u \in H^s(\Omega) \cap H_0^1(\Omega)$. Let U be the SDFEM solution obtained with weights ρ_K given by $\rho_K = h_K/p_K$. Assume (2.13) and (4.8). Then we have*

$$\|u - U\|_{SD} \leq C\left\{\sum_{K\in\mathcal{T}} \frac{h_K^{2\nu_K-2}}{p_K^{2s-2}}\|u\|^2_{H^s(K)}(\varepsilon + \frac{h_K}{p_K})\right\}^{\frac{1}{2}}$$

with $\nu_K = \min(p_K + 1, s)$.

Proof: Due to assumption (4.8) we can bound the term $\delta_K\rho_K\varepsilon^2\frac{p_K^2}{h_K^2}$ in (5.14) by $C\frac{h_K^2}{p_K^6}$. Hence, from (5.13) and (5.14) we get that

$$\|U - Iu\|^2_{SD} \leq C\sum_{K\in\mathcal{T}} \frac{h_K^{2\nu_K-2}}{p_K^{2s-2}}\|u\|^2_{H^s(K)}(\varepsilon + \frac{h_K}{p_K}).$$

The claim follows now by an application of the triangle inequality. □

Remark 5.9 If the mesh $\mathcal{T}$ is quasiuniform, i.e. $h_K \sim h$, and if we use a uniform polynomial degree p on all elements, i.e. $p_K = p$, we get

$$\|u - U\|_{SD} \leq C \frac{h^{(\min(p+1,s)-1)}}{p^{(s-1)}} (\varepsilon^{\frac{1}{2}} + (\frac{h}{p})^{\frac{1}{2}}) \|u\|_{H^s(K)}.$$

Remark 5.10 The error estimate for the SDFEM in Proposition 5.8 and Remark 5.9 is half a power of h/p away from being quasi-optimal [23]. For the h-version of the SDFEM this is a well known fact, which is extended in Proposition 5.8 to the p-version of the SDFEM.

6. Numerical Examples

In this section we confirm the theoretical results in a series of numerical examples.

6.1. Model Problems

We consider two convection-diffusion model problems of the form (2.1), M1 and M2, where we explicitly prescribe the exact solution u:

Model Problem M1: Here, $\Omega = (-1, 0) \times (-1, 1)$, $\vec{a}(x) = (1, 0)^t$, $b(x) = 1$ and the right-hand side is chosen as $f(x) = c_1(\varepsilon)x_1 + c_1 + c_2$ with $c_1(\varepsilon) = \exp(\frac{-(1+\sqrt{1+4\varepsilon})}{2\varepsilon}) - 1$ and $c_2 = -1$. The exact solution is

$$u(x) = \exp(\frac{1 + \sqrt{1 + 4\varepsilon}}{2\varepsilon} x_1) + c_1(\varepsilon)x_1 + c_2.$$

This solution satisfies (2.1) with zero Dirichlet conditions at the boundaries $\{x = -1\}$, $\{x = 0\}$ and symmetry conditions at $\{y = -1\}$, $\{y = 1\}$. It has an exponential boundary layer along the right side of Ω. u is essentially one dimensional and we use this model problem to confirm the numerical results of [17].

Model Problem M2: Here, $\Omega = (0, 1)^2$, $a(x) = (1, 1)^t$, $b(x) = 1$ and

$$\begin{aligned} f(x) \;=\; & c_1(x)x_2 - c_1(x)c_2(x)x_2 + x_1c_2(x) - x_1c_1(x)c_2(x) + x_2 - x_2c_2(x) + x_1 \\ & -x_1c_1(x) + x_1x_2 - x_1x_2c_2(x) - x_1c_1(x)x_2 + x_1c_1(x)c_2(x)x_2 \end{aligned}$$

with $c_1(x) = \exp((x_1 - 1)/\varepsilon)$ and $c_2(x) = \exp((x_2 - 1)/\varepsilon)$. The exact solution is

$$u(x) = x_1x_2(1 - \exp(-(1 - x_1)/\varepsilon))(1 - \exp(-(1 - x_2)/\varepsilon)).$$

It satisfies (2.1), the zero Dirichlet boundary conditions in (2.2) and has two exponential boundary layers along the top and right side of Ω.

To discretize these equations by the *hp*-SDFEM in (2.7) we use the Fortran 90 code HP90, a general *hp*-FEM framework for Finite Element implementations (see [2]). The SDFEM parameters are chosen as in (2.11), i.e., $\rho_K = h_K/p_K^\alpha$ with the constant α still at our disposal. We are mainly interested in $\alpha = 1$ and $\alpha = 2$. In addition, we will also compare the Galerkin approach (2.6) with the SDFEM (2.7) which can easily be done by setting $\delta_K = 0$ for all $K \in \mathcal{T}$.

6.2. Results for M1

We present the results for the model problem M1: We consider first the SDFEM and Galerkin performance for $\varepsilon = 0.1$ on a four element mesh given by an equidistant partition in x-direction. For this large value of ε the layer is of course very weak and the element on the right resolves it already. We measure the relative H^1 error in the element on the left side, i.e., in the element that is farthest away from the boundary layer. From Figure 3 we see that the Galerkin method performs best followed by the SDFEM with $\rho_K = h_K/p_K^2$. We observe that $\rho_K = h_K/p_K$ is not the correct choice for the SDFEM parameter, in the case that ε is small compared to h_K and $1/p_K$, just as asserted in in Proposition 4.3.

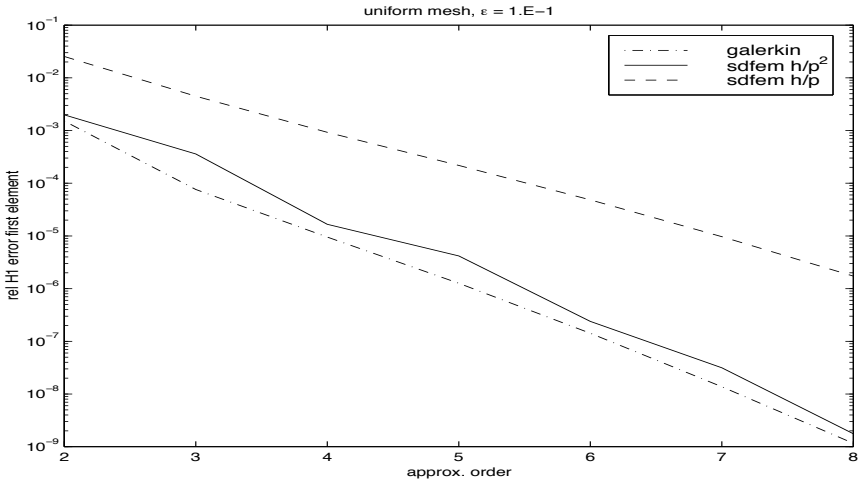

Figure 3: M1: Local H^1 error upstream on uniform 4 element mesh.

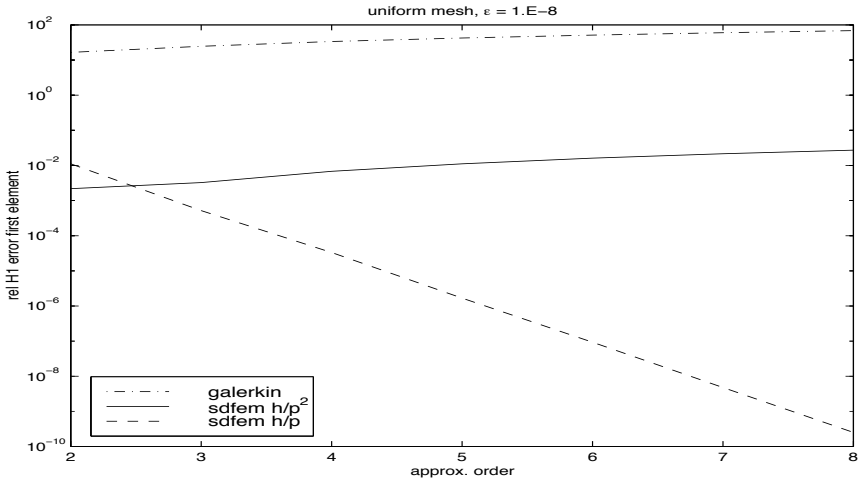

Figure 4: M1: Local H^1 error upstream on uniform 4 element mesh.

In Figure 4 we perform the same experiment on exactly the same mesh with $\varepsilon = 10^{-8}$. This time the behaviour of the three curves is different. We clearly see that the Galerkin method does not give any reasonable solution. The SDFEM with $\rho_K = h_K/p_K$ performs best and indeed converges exponentially, whereas the SDFEM with $\rho_K = h_K/p_K^2$ diverges

and the error is several orders of magnitude worse. Therefore, for ε small compared to h_K and $1/p_K$ the stabilization parameter should be chosen as $\rho_K = h_K/p_K$.
The pointwise error along the line $y = 0$ through Ω for the three methods is shown in Figure 5 and we clearly see that the SDFEM error with $\rho_K = h_K/p_K$ decays exponentially in the upstream direction. The decay with $\rho_K = h_K/p_K^2$ is still exponential outside the boundary layer but again several orders of magnitude worse.

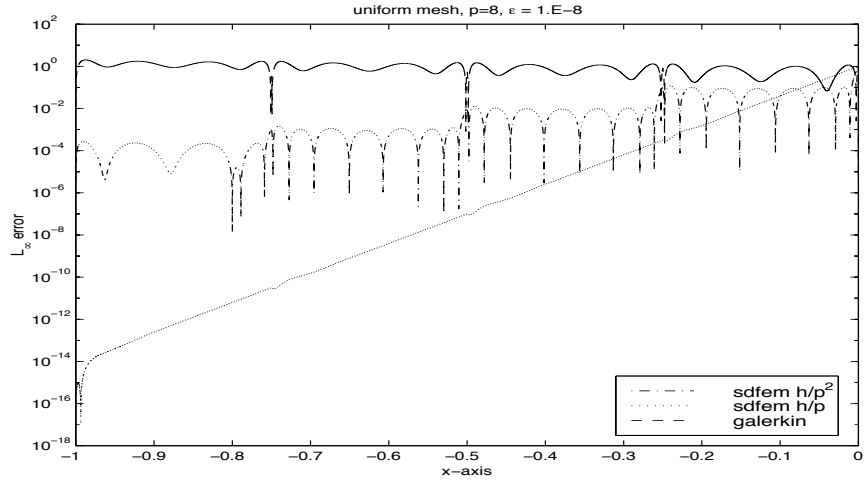

Figure 5: M1: Pointwise error on uniform 4 element mesh.

Of interest is now the question for which parameter α in the h/p^α factor the performance of the SDFEM is best. For $\varepsilon = 10^{-8}$ we investigate this on a quasiuniform mesh which is not aligned with the coordinate axes. Again, we measure the relative H^1 error in the element farthest away from the boundary layer. The results in Figure 6 indicate the superior performance of the SDFEM for $\alpha = 1$, which is consistent with one dimensional numerical results in [17] and with the theoretical analysis for the limiting case $\varepsilon = 0$ in [5]. In particular, we note again that $\alpha = 2$ is not the correct choice for small values of ε.

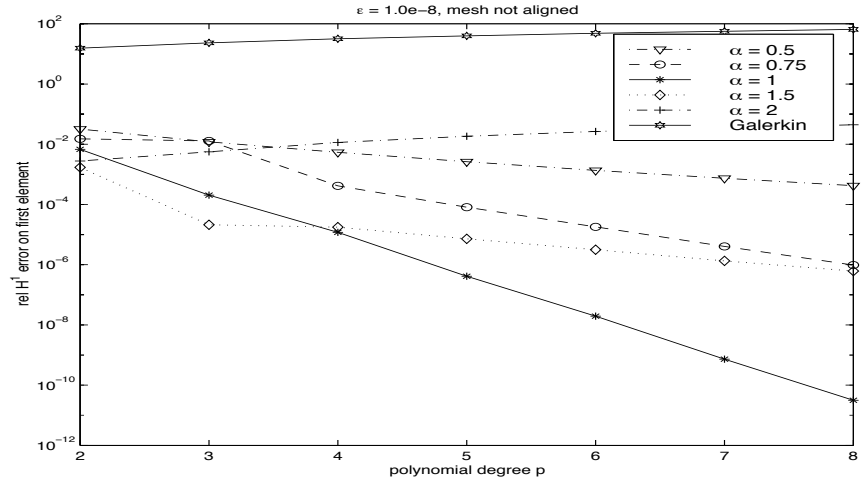

Figure 6: M1: Local H^1 error upstream on quasiuniform non-aligned 16 element mesh.

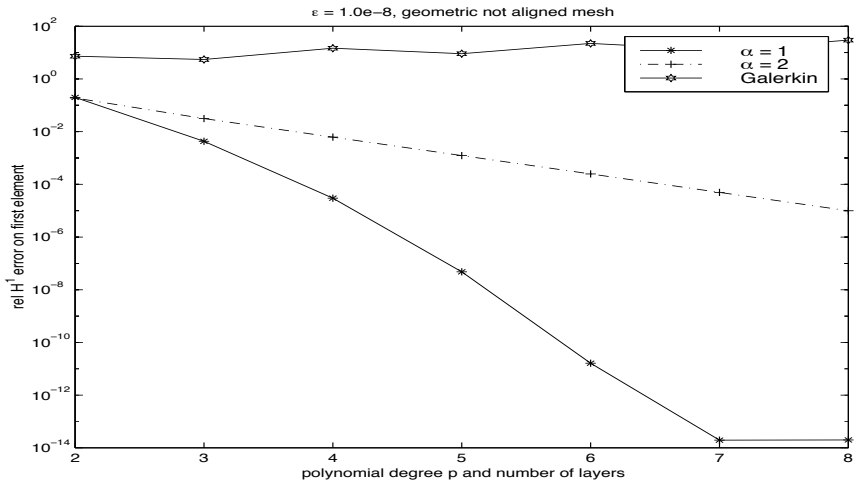

Figure 7: M1: Local H^1 error upstream on geometrically graded non-aligned mesh.

In Figure 7 we show the performance for M1 on geometric boundary layer meshes. We start with $p = 2$ on a four element mesh that is not aligned with the flow. We insert geometrically graded layers towards the boundary $\{x = 0\}$ and also uniformly increase p. We show the results for the Galerkin method, which does not converge in the range of $p = 1, \ldots, 8$, for $\rho_K = h_K/p_K^2$ and for $\rho_K = h_K/p_K$. In the last case we see again a superior performance.

6.3. Results for M2

The results for M1 are now confirmed for M2. We use here a uniform mesh with 16 elements that are either aligned or slightly perturbed. These meshes are shown in Figure 8.

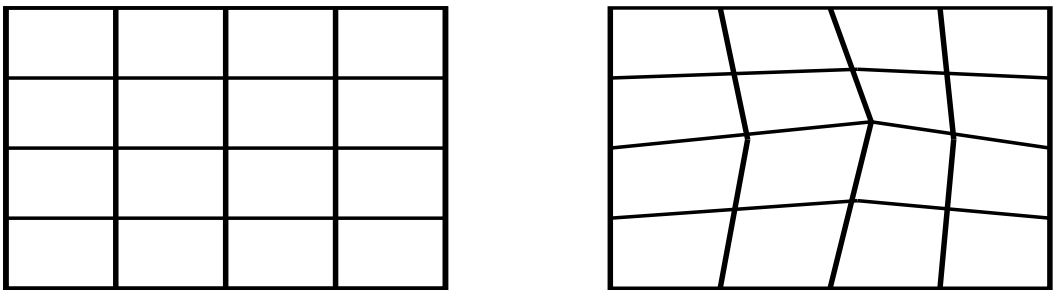

Figure 8: Uniform aligned mesh and non-aligned mesh.

We again perform similar experiments and present in Figures 9 and 10 the local relative H^1 error in the element that has largest distance to the boundary layers. The results are for $\varepsilon = 10^{-8}$ and, as expected from the previous results, the SDFEM with $\rho_K = h_K/p_K$ performs best and converges exponentially. It is remarkable that the SDFEM with $\rho_K = h_K/p_K^2$ diverges in the practical range of p.
Finally, we present the global relative H^1 error on a boundary layer mesh with anisotropic needle elements of width 10ε (this mesh is essentially a tensor product construction corresponding to the patch (P2) in order to resolve the layers at both outflow boundaries $x = 1$ and $y = 1$). From Figure 11 we see that the performance of the Galerkin method is superior in this case, whereas the SDFEM does perform rather poorly for $\rho_K = h_K/p_K$. There is no

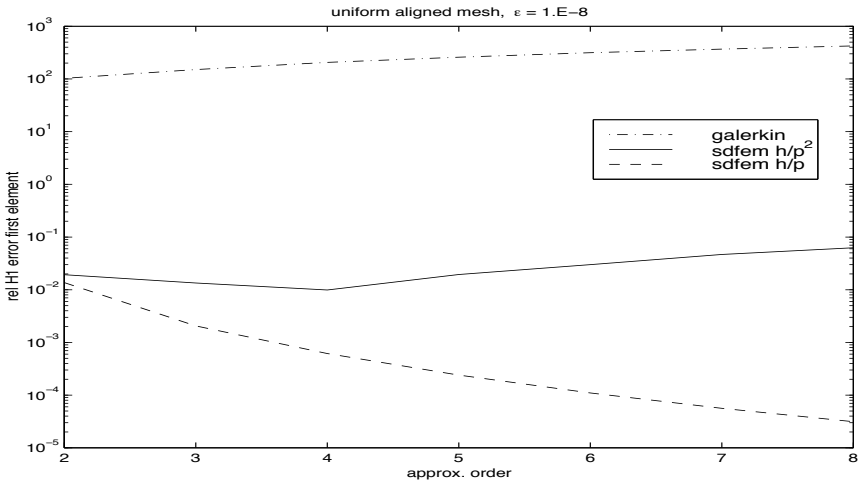

Figure 9: M2: Local H^1 error upstream on aligned mesh.

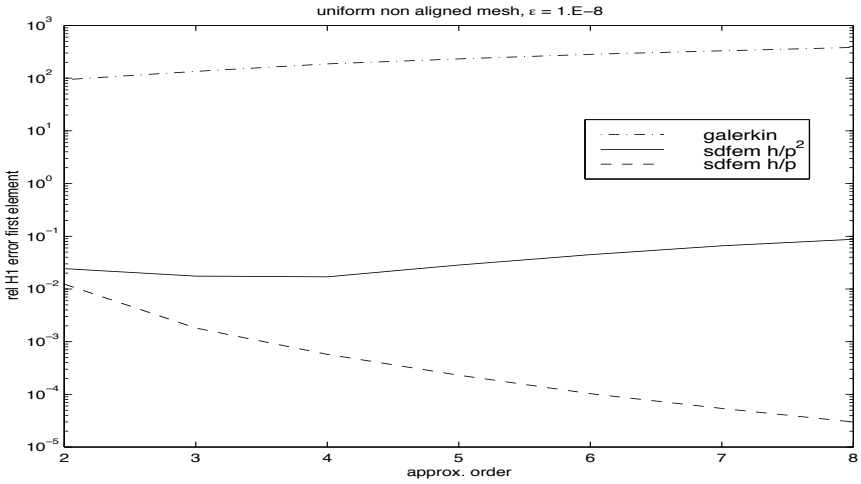

Figure 10: M2: Local H^1 error upstream on non-aligned mesh.

need for the SDFEM stabilization if the mesh already resolves the layers. However, we get exponential convergence in all cases as predicted in Section 5.

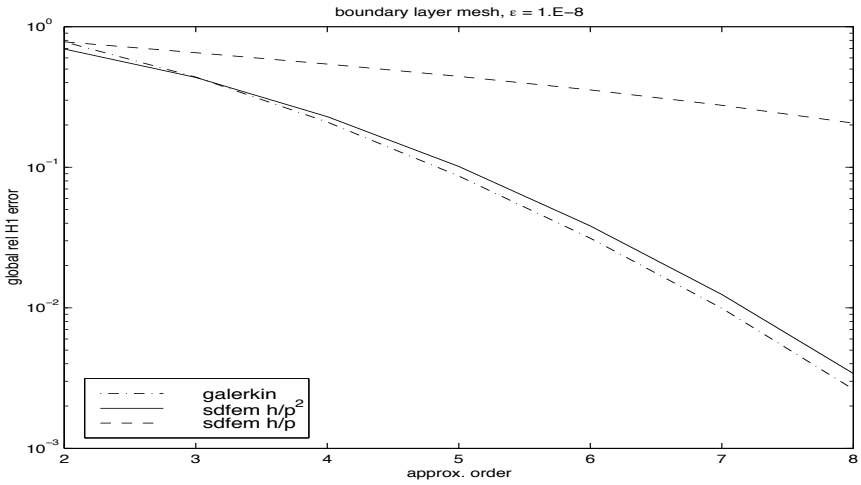

Figure 11: M2: Global H^1 error on boundary layer mesh.

A. Proof of Theorems 3.5, 3.7, 3.8

A.1. Approximation in One Dimension

We start by introducing the following two projectors: Let $\mathcal{T}$ be an arbitrary mesh on $(0,1)$. Then we introduce

1. $i_p^x : C([0,1]) \to S^p(\mathcal{T})$ is the piecewise Gauss-Lobatto interpolation operator.
2. Let $\overline{x} \in (0,1)$ an arbitrary mesh point of $\mathcal{T}$. Then the projector $P_p^x : C([0,1]) \to S^p(\mathcal{T})$ is defined by

$$P_p^x u(x) := \begin{cases} (i_p^x u)(x) - \dfrac{x}{\overline{x}} u(\overline{x}) & \text{on } (0,\overline{x}) \\ \dfrac{x-\overline{x}}{1-\overline{x}} u(1) & \text{on } (\overline{x},1). \end{cases}$$

We have the following L^∞ stability result for these two interpolation operators:

Lemma A.1 *There is $C > 0$ independent of p, the mesh $\mathcal{T}$ and the mesh point $\overline{x} \in (0,1)$ such that there holds*

$$\|i_p^x u\|_{L^\infty((0,1))} + \|P_p^x u\|_{L^\infty((0,1))} \le C(1+\ln p)\|u\|_{L^\infty((0,1))} \qquad \forall u \in C([0,1]).$$

Proof: The stability result for the Gauss-Lobatto interpolation operator i_p^x was proved in [25]. That result implies readily the stability of the operator P_p^x. □

In analogy to condition (3.5) functions of boundary layer type satisfy in one dimension:

$$|\partial_x^n u(x)| \le C\gamma^n \max\{l^{-1}, n\}^n e^{-dx/l} \quad \forall n \in \mathbb{N}_0, \quad x \in (0,1). \tag{A.1}$$

Robust exponential approximations of such functions can be achieved with the projector P_p^x provided that the point $\overline{x}$ can be chosen such that $\overline{x} = O(pl)$ is a mesh point.

Lemma A.2 *Let u satisfy (A.1). Then there are C, σ, $\kappa_0 > 0$ independent of l and p such that the following holds: Let $\mathcal{T}$ be an arbitrary mesh on $(0,1)$ and assume that for some $\kappa \in (0,\kappa_0)$ the point $\overline{x} := \min\{1/2, \kappa pl\}$ is a mesh point of $\mathcal{T}$. Then the projector $P_p^x u$ (defined with this choice of the point $\overline{x}$) satisfies*

$$\begin{aligned} \kappa pl\|(u-P_p^x u)'\|_{L^2((0,1))} + \|u-P_p^x u\|_{L^2((0,1))} &\le Cl^{1/2}e^{-\sigma\kappa p}, \\ \kappa pl\|(u-P_p^x u)'\|_{L^\infty(I_i)} + \|u-P_p^x u\|_{L^\infty(I_i)} &\le Ce^{-\sigma\kappa p} \qquad \text{for } I_i \subset (0,\overline{x}), \\ \kappa pl\|(u-P_p^x u)'\|_{L^\infty(I_i)} + \|u-P_p^x u\|_{L^\infty(I_i)} &\le Ce^{-\sigma x_i/l} \qquad \text{for } I_i = (x_i, x_{i+1}) \subset (\overline{x},1). \end{aligned}$$

Proof: This result is proved as Lemma 2.4 in [17]. Note that the special case of a two-element mesh $\mathcal{T} = \{(0,\kappa pl),(\kappa pl,1)\}$ is contained as a special case. □

A.2. Two Dimensional Approximation Results

Due to Lemma 3.4, we can restrict our attention in the two dimensional setting to a reference configuration, and for the remainder of this section, we will assume that the function u is defined on the closed reference square $S = [0,1]^2$ and satisfies there the growth conditions in (3.5). We consider tensor product meshes on S in order to be able to exploit our one dimensional results. To that end, we denote by i_p^y the one dimensional (piecewise) Gauss-Lobatto interpolation operator as defined above but acting on the y-variable instead of the x-variable. We have:

Lemma A.3 *Let u satisfy (3.5). Then there are C, σ, $\kappa_0 > 0$ independent of p and l such that following holds: Let $\mathcal{T}_x$, $\mathcal{T}_y$ be arbitrary meshes on $(0,1)$ and let $\mathcal{T} := \mathcal{T}_x \times \mathcal{T}_y$ be the tensor product mesh on S. Assume that for some $\kappa \in (0, \kappa_0)$ the point $\overline{x} := \min\{1/2, \kappa pl\}$ is a mesh point of $\mathcal{T}_x$. Then the interpolant $\pi_p := (i_p^y \circ P_p^x)u = (P_p^x \circ i^y)u \in S^p(\mathcal{T})$ satisfies*

$$\begin{aligned} \kappa pl\|\nabla(u-\pi_p)\|_{L^2(S)} + \|u-\pi_p\|_{L^2(S)} &\leq Cl^{1/2}(1+\ln p)e^{-\sigma\kappa p}, \\ \kappa pl\|\nabla(u-\pi_p)\|_{L^\infty(I_x\times I_y)} + \|u-\pi_p\|_{L^\infty(I_x\times I_y)} &\leq C(1+\ln p)e^{-\sigma\kappa p} \quad \text{for } I_x \subset (0,\overline{x}) \end{aligned}$$

and

$$\kappa pl\|\nabla(u-\pi_p)\|_{L^\infty(I_x\times I_y)} + \|u-\pi_p\|_{L^\infty(I_x\times I_y)} \leq C(1+\ln p)e^{-\sigma x_i/l}$$

for $I_x = (x_i, x_{i+1}) \subset (\overline{x}, 1)$. In the last two estimates, I_y may be an arbitrary element of $\mathcal{T}_y$.

Proof: We will only show the L^∞-bounds. Let $I_x = (x_i, x_{i+1})$, I_y be elements of $\mathcal{T}_x$, $\mathcal{T}_y$. We have

$$\begin{aligned} \|u-\pi_p\|_{L^\infty(I_x\times I_y)} &\leq \|u - i_p^y u\|_{L^\infty(I_x\times I_y)} + \|i_p^y(u - P_p^x u)\|_{L^\infty(I_x\times I_y)} \\ &\leq \|u - i_p^y u\|_{L^\infty(I_x\times I_y)} + C(1+\ln p)\|u - P_p^x u\|_{L^\infty(I_x\times I_y)} \end{aligned}$$

by the one-dimensional stability result Lemma A.1. Standard polynomial approximation results (cf., e.g., [15]) give the existence of C, $\sigma > 0$ depending only on C and γ of (3.5) such that

$$\|\partial_y(u - i_p^y u)\|_{L^\infty(I_x\times I_y)} + \|u - i_p^y u\|_{L^\infty(I_x\times I_y)} \leq Ce^{-dx_i/l}e^{-\sigma p}. \tag{A.2}$$

Using this and the one dimensional results of Lemma A.2 we arrive at

$$\begin{aligned} \|u-\pi_p\|_{L^\infty(I_x\times I_y)} &\leq C(1+\ln p)e^{-\sigma\kappa p} \qquad \text{if } I_x \subset (0,\overline{x}), \\ \|u-\pi_p\|_{L^\infty(I_x\times I_y)} &\leq C(1+\ln p)e^{-\sigma x_i/l} \qquad \text{if } I_x \subset (\overline{x},1). \end{aligned}$$

For the estimates on the derivatives, we proceed similarly. We have, using the additional fact that ∂_y and P_p^x commute,

$$\begin{aligned} &\|\partial_y(u - i_p^y P_p^x u)\|_{L^\infty(I_x\times I_y)} \leq \|\partial_y(u - P_p^x u)\|_{L^\infty(I_x\times I_y)} + \|\partial_y(P_p^x u - P_p^x i_p^y u)\|_{L^\infty(I_x\times I_y)} \\ &\leq \|(\partial_y u) - P_p^x(\partial_y u)\|_{L^\infty(I_x\times I_y)} + \|P_p^x(\partial_y(u - i_p^y u))\|_{L^\infty(I_x\times I_y)} \\ &\leq \|(\partial_y u) - P_p^x(\partial_y u)\|_{L^\infty(I_x\times I_y)} + C(1+\ln p)\|\partial_y(u - i_p^y u)\|_{L^\infty(I_x\times I_y)}. \end{aligned}$$

These last two terms can be estimated in the desired fashion using Lemma A.2. Finally, for the derivative in the x-direction, we have

$$\begin{aligned} &\|\partial_x(u - i_p^y P_p^x u)\|_{L^\infty(I_x\times I_y)} \leq \|\partial_x(u - i_p^y u)\|_{L^\infty(I_x\times I_y)} + \|\partial_x(i_p^y u - i_p^y P_p^x u)\|_{L^\infty(I_x\times I_y)} \\ &\leq \|(\partial_x u) - i_p^y(\partial_x u)\|_{L^\infty(I_x\times I_y)} + \|i_p^y(\partial_x(u - P_p^x u))\|_{L^\infty(I_x\times I_y)} \\ &\leq \|(\partial_x u) - i_p^y(\partial_x u)\|_{L^\infty(I_x\times I_y)} + C(1+\ln p)\|\partial_x(u - P_p^x u)\|_{L^\infty(I_x\times I_y)}. \end{aligned}$$

It it now easy to see from standard approximation results that there holds

$$\|(\partial_x u) - i_p^y(\partial_x u)\|_{L^\infty(I_x\times I_y)} \le Cl^{-1}e^{-dx_i/l}e^{-\sigma p}.$$

Next, $\|\partial_x(u - P_p^x u)\|_{L^\infty(I_x\times I_y)}$e can be bounded again by Lemma A.2. This completes the proof. □

We note that Lemma A.3 proves Theorem 3.5. Lemma A.3 is also the basis for the proof of Theorem 3.7.

Proof of Theorem 3.7 : The key observation to employ the preceding lemma is that by our assumption that $q^L \approx l$ there is $k \in \{0,\dots,L\}$ such that $q^{k+1} \le \kappa_0 pl \le q^k$. Hence, there is always a mesh point in $\mathcal{T}_x$ of the form $\overline{x} = \kappa pl$ with $\kappa \in (\kappa_0 q, \kappa_0]$. In order to simplify the notation for the remainder of this proof, we assume that $q^k = \kappa_0 pl$. The first two estimates therefore follow immediately. It remains to see that the last two ones hold. For the elements $I_i = (x_i, x_{i+1})$ of $\mathcal{T}_x$ we write $h_i := x_{i+1} - x_i$ and similarly, we write h_j for the length of the j-th element I_j of $\mathcal{T}_y$. We now estimate for the elements near $x = 0$ with Lemma A.3

$$\sum_{i=k}^{L+1}\sum_j \frac{h_i h_j}{l} l^2 \|\nabla(u-\pi_p)\|^2_{L^\infty(I_i\times I_j)} \;\le\; C\sum_{i=k}^{L+1}\frac{h_i}{l}e^{-\sigma p} \le C\frac{\kappa_0 pl}{l}e^{-\sigma p} \le Ce^{-\sigma p}.$$

Now, for the elements that are "far" from $x = 0$, we have for $i \le k$, by the assumption that the mesh is graded geometrically towards $x = 0$, that there holds $h_i \sim x_i$ with constants independent of i and l. Hence, from Lemma A.3

$$\sum_{i=0}^{k}\sum_j \frac{h_i h_j}{l} l^2 \|\nabla(u-\pi_p)\|^2_{L^\infty(I_i\times I_j)} \le C\sum_{i=0}^{k}\frac{x_i}{l}e^{-\sigma x_i/l} \le C\sum_{i=0}^{k} e^{-\sigma' x_i/l} \le Ce^{-\sigma p}.$$

This completes the proof of the third estimate. For the last one, we proceed similarly. We have

$$\begin{aligned}\sum_{i=k}^{L+1}\sum_j \min\{h_i,h_j\}\|\nabla(u-\pi_p)\|^2_{L^2(I_i\times I_j)} &\le \sum_{i=k}^{L+1} h_i \|\nabla(u-\pi_p)\|^2_{L^2(S)}\\ &\le C\sum_{i=k}^{L+1} h_i l^{-1}e^{-\sigma p} \le C\frac{\kappa_0 pl}{l}e^{-\sigma p} \le Ce^{-\sigma p}\end{aligned}$$

and finally, again as $h_i \sim x_i$ for $i \le k$:

$$\begin{aligned}\sum_{i=0}^{k}\sum_j \min\{h_i,h_j\}\|\nabla(u-\pi_p)\|^2_{L^2(I_i\times I_j)} &\le \sum_{i=0}^{k}\sum_j h_i^2 h_j \|\nabla(u-\pi_p)\|^2_{L^\infty(I_i\times I_j)}\\ &\le C\sum_{i=0}^{k} h_i^2 l^{-2}e^{-\sigma x_i/l} \le C\sum_{i=0}^{k} e^{-\sigma x_i/l} \le Ce^{-\sigma p}.\end{aligned}$$

This completes the proof of Theorem 3.7. □

The proof of Theorem 3.8 is a straightforward extension of the arguments above.

References

[1] I. Babuška and M. Suri, *The p and h-p versions of the finite element method, basic principles and properties*, SIAM Review **36** (1994), 578–632.

[2] L. Demkowicz, K. Gerdes, C. Schwab, A. Bajer and T. Walsh, *HP90: A general & flexible Fortran 90 hp-FE code*, Computing and Visualization in Science **1** (1998), 145-163.

[3] D. Funaro, *Spectral Elements for Transport-Dominated Equations*, Springer Verlag, 1997.

[4] P. Hansbo, *Adaptivity and streamline diffusion procedures in the finite element method*, PhD thesis, Chalmers University of Technology, Göteborg, 1989.

[5] P. Houston, C. Schwab and E. Süli, *Stabilized hp-finite element methods for first-order hyperbolic problems*, Report 98/14, Oxford Computing Laboratory, 1998.

[6] T.J. Hughes and A. Brooks, *A multidimensional upwind scheme with no crosswind diffusion*, AMD **34**, Finite element methods for convection dominated flows, ed.: T.J. Hughes, ASME, New York, 1979.

[7] T.J. Hughes and A. Brooks, *A theoretical framework for Petrov-Galerkin methods with discontinuous weighting functions, Applications to the streamline-upwind procedure*, Finite Elements in Fluids **4** (1982), eds.: R.H. Gallagher et al., Wiley, 1982.

[8] T.J. Hughes, L. Franca and M. Balestra, *A new finite element formulation for computational fluid dynamics: V. Circumventing the Babuška-Brezzi condition: A stable Petrov-Galerkin formulation of the Stokes problem accomodating equal-order interpolations*, Comput. Methods Appl. Mech. Engrg. **59** (1986), 85–99.

[9] D. Gilbarg and N.S. Trudinger. *Elliptic Partial Differential Euations of Second Order.* Grundlagen der mathematischen Wissenschaften 224. Springer Verlag 1977.

[10] C. Johnson, *Numerical Solution of Partial Differential Equations by the Finite Element Method*, Cambridge University Press, 1987.

[11] C. Johnson, *Streamline diffusion methods for problems in fluid mechanics*, Finite Elements in Fluids **6** (1985), eds.: R.H. Gallagher et al., Wiley, 1985.

[12] C. Johnson, U. Nävert and J. Pitkäranta, *Finite element methods for linear hyperbolic problems*, Comput. Methods Appl. Mech. Engrg. **45** (1984), 285–312.

[13] C. Johnson and J. Saranen, *Streamline diffusion methods for the incompressible Euler and Navier-Stokes equations*, Math. Comp. **47** (1986), 1–18.

[14] C. Johnson, A. Schatz and L. Wahlbin, *Crosswind Smear and Pointwise Errors in the Streamline Diffusion Finite Element Method*, Math. Comp. **49** (1987), 25–38.

[15] J.M. Melenk, *On the robust exponential convergence of finite element methods for problems with boundary layers*, IMA J. Num. Anal. **17** (1997), 577–602.

[16] J.M. Melenk and C. Schwab, *An hp finite element method for convection-diffusion problems in one dimension*, IMA J. Numer. Anal. **19** (1999), 425-453.

[17] J.M. Melenk and C. Schwab, *The hp Streamline Diffusion Finite Element Method for convection-dominated problems in one dimension*, East-West J. Numer. Math. **7** (1999), 31-60.

[18] J.M. Melenk and C. Schwab, *hp-FEM for reaction-diffusion equations. I: Robust Exponential Convergence*, SIAM J. Numer. Anal. **35** (1998), 1520-1557.

[19] J.M. Melenk and C. Schwab, *Analytic regularity for a singularly perturbed problem*, SIAM J. Math. Anal. **30** (1999), 379–400.

[20] J.J.H. Miller, E. O'Riordan and G.I. Shishkin, *Fitted Numerical Methods for Singular Perturbation Problems*, World Scientific Publishers, Singapore, 1996.

[21] K.W. Morton, *Numerical solution of convection-diffusion problems*, Oxford University Press, 1995.

[22] H.G. Roos, M. Stynes and L. Tobiska, *Numerical Methods for Singularly Perturbed Differential Equations*, Springer Verlag Heidelberg, New York, 1995.

[23] C. Schwab, *p- and hp-Finite Element Methods*, Oxford University Press, 1998.

[24] C. Schwab and M. Suri, *The p and hp versions of the finite element method for problems with boundary layers*, Math. Comp. **65** (1996), 1403–1429.

[25] B. Sündermann, *Lebesgue constants in Lagrangian interpolation at the Fekete points*, Ergebnisberichte der Lehrstühle Mathematik III und VIII (Angewandte Mathematik) **44**, Universität Dortmund, 1980.

[26] M. Stynes and L. Tobiska, *Analysis of Streamline-Diffusion-Type Methods on Arbitrary and Shishkin Meshes*, Preprint 97-03, Dept. of Math., University College, Cork, Ireland, 1997.

[27] C. Schwab, M. Suri and C.A. Xenophontos, *Boundary Layer Approximation by Spectral/ hp Methods*, Houston J. Math. Spec. Issue of ICOSAHOM 1995 Conference, eds.: A.V. Illin and L.R. Scott, 501-508, 1996.

[28] S.-D. Shi and R.B. Kellogg, *Asymptotic analysis of a singular perturbation problem*, SIAM Math. Anal. **18** (1987) 1467–1511.

[29] R. Stenberg and L. Franca, *Error analysis of some Galerkin least squares methods for the elasticity equations*, SIAM J. Numer. Anal. **28** (1991), 1680–1697.

[30] L. Tobiska and R. Verfürth, *Analysis of a streamline diffusion finite element method for the Stokes and Navier-Stokes equations*, SIAM J. Numer. Anal. **33** (1996), 107–127.

[31] G. Zhou, *Local L^2 error analysis of the Streamline Diffusion FE-Method for nonstationary hyperbolic systems*, RAIRO **25** (1995), 577–603.

[32] G. Zhou, *Local Pointwise error estimates for the Streamline Diffusion Method applied to nonstationary hyperbolic problems*, East-West J. Num. Math. **3** (1995), 217–235.

[33] G. Zhou and R. Rannacher, *Pointwise Superconvergence of the Streamline Diffusion Finite Element Method*, Num. Meth. PDEs **12** (1996), 123–145.

Research Reports

No.	Authors	Title
99-17	K. Gerdes, J.M. Melenk, D. Schötzau, C. Schwab	The *hp*-Version of the Streamline Diffusion Finite Element Method in Two Space Dimensions
99-16	R. Klees, M. van Gelderen, C. Lage, C. Schwab	Fast numerical solution of the linearized Molodensky problem
99-15	J.M. Melenk, K. Gerdes, C. Schwab	Fully Discrete *hp*-Finite Elements: Fast Quadrature
99-14	E. Süli, P. Houston, C. Schwab	*hp*-Finite Element Methods for Hyperbolic Problems
99-13	E. Süli, C. Schwab, P. Houston	*hp*-DGFEM for Partial Differential Equations with Nonnegative Characteristic Form
99-12	K. Nipp	Numerical integration of differential algebraic systems and invariant manifolds
99-11	C. Lage, C. Schwab	Advanced boundary element algorithms
99-10	D. Schötzau, C. Schwab	Exponential Convergence in a Galerkin Least Squares *hp*-FEM for Stokes Flow
99-09	A.M. Matache, C. Schwab	Homogenization via *p*-FEM for Problems with Microstructure
99-08	D. Braess, C. Schwab	Approximation on Simplices with respect to Weighted Sobolev Norms
99-07	M. Feistauer, C. Schwab	Coupled Problems for Viscous Incompressible Flow in Exterior Domains
99-06	J. Maurer, M. Fey	A Scale-Residual Model for Large-Eddy Simulation
99-05	M.J. Grote	Am Rande des Unendlichen: Numerische Verfahren für unbegrenzte Gebiete
99-04	D. Schötzau, C. Schwab	Time Discretization of Parabolic Problems by the hp-Version of the Discontinuous Galerkin Finite Element Method
99-03	S.A. Zimmermann	The Method of Transport for the Euler Equations Written as a Kinetic Scheme
99-02	M.J. Grote, A.J. Majda	Crude Closure for Flow with Topography Through Large Scale Statistical Theory
99-01	A.M. Matache, I. Babuška, C. Schwab	Generalized *p*-FEM in Homogenization
98-10	J.M. Melenk, C. Schwab	The *hp* Streamline Diffusion Finite Element Method for Convection Dominated Problems in one Space Dimension
98-09	M.J. Grote	Nonreflecting Boundary Conditions For Electromagnetic Scattering
98-08	M.J. Grote, J.B. Keller	Exact Nonreflecting Boundary Condition For Elastic Waves